ISTANBUL TECHNICAL UNIVERSITY ★ GRADUATE SCHOOL

SURFACE MODIFIED CELLULOSE NANOCRYSTAL INCORPORATED NANOCOMPOSITES

M.Sc. THESIS

Onur Nuri ARSLAN

Department of Materials Science and Engineering

Material Science and Engineering Graduate Programme

SEPTEMBER 2022

ISTANBUL TECHNICAL UNIVERSITY ★ GRADUATE SCHOOL

SURFACE MODIFIED CELLULOSE NANOCRYSTAL INCORPORATED NANOCOMPOSITES

M.Sc. THESIS

Onur Nuri ARSLAN
(521201009)

Department of Materials Science and Engineering

Material Science and Engineering Graduate Programme

Thesis Advisor: Assoc. Prof. M. Reza NOFAR

SEPTEMBER 2022

İSTANBUL TEKNİK ÜNİVERSİTESİ ★ LİSANSÜSTÜ EĞİTİM ENSTİTÜSÜ

YÜZEY MODİFİYE SELÜLOZ NANOKRİSTAL KATKILI NANOKOMPOZİTLER

YÜKSEK LİSANS TEZİ

Onur Nuri ARSLAN
(521201009)

Malzeme Bilimi ve Mühendisliği Anabilim Dalı

Malzeme Bilimi ve Mühendisliği Programı

Tez Danışmanı: Doç. Dr. M. Reza NOFAR

EYLÜL 2022

Onur Nuri ARSLAN, a M.Sc. student of İTU Graduate School student ID 521201009, successfully defended the thesis/dissertation entitled "SURFACE MODIFIED CELLULOSE NANOCRYSTAL INCORPORATED NANOCOMPOSITES", which he prepared after fulfilling the requirements specified in the associated legislations, before the jury whose signatures are below.

Thesis Advisor :	**Assoc. Prof. M.Reza NOFAR** Istanbul Technical University	……..
Jury Members :	**Prof. Dr. Burçak KARAGÜZEL KAYAOĞLU** Istanbul Technical University	……..
	Prof. Dr. Ali DURMUŞ Istanbul University- Cerrahpaşa	……..

Date of Submission : 07 August 2022
Date of Defense : 02 September 2022

To my family,

FOREWORD

First and foremost, I would like to express my gratitude to my supervisor Assoc. Prof. M. Reza NOFAR for his invaluable support, guidance and encouragements. The values he brought to me will be valuable items that I will always carry with me in my academic life. It was an unique opportunity to work with him.

I would like to thank Dr. Yonca Alkan GÖKSU at Istanbul Technical University for her support, guidance and encouragements. Also, I feel grateful for sharing her valuable chemistry knowledge with me.

I am also grateful to Research Assistant Aylin BEKEM for sharing her knowledge and not leaving me alone in laboratory studies.

I would like to thank MSc. Dilara GÜNTÜRKÜN for her valued friendship and support as a teammate.

I would also like to thank Research Assistant Burcu ÖZDEMİR for helping runnig rheological analysis and her supports in difficult times.

I express my sincere appreciation to Oğuzhan ÖZENÇ, Berkay EZGÜ and Ceren ÖZSALTIK for their precious friendship and support.

Finally, I would like to dedicate my thesis to my family: my mother Nurgül ARSLAN, my father Samir ARSLAN, my brother Ozan ARSLAN, my cousin Simge ATEŞ, my grandmother Türkan MADAN and my grandfather Ali MADAN.

I would like to acknowledge the financial supports from Istanbul Technical University Scientific Research Project (ITU-BAP) – Master Thesis Project with the project number of 43069.

August 2022

Onur Nuri ARSLAN
(Metallurgical and Materials Engineer)

TABLE OF CONTENTS

Page

ABBREVIATIONS

AFM **:** Atomic Force Microscope
APTES **:** 3-aminopropyltriethoxysilane
ATR-IR **:** Attenuated total reflection infrared spectroscopy
$C_{18}H_{37}NCO$ **:** n-octadecyl isocyanate
CAN : Ceric Ammonium Nitrate
CNC **:** Cellulose nanocrystal
CNC-g-PGMA: CNC grafted PGMA
CNS **:** Corn nanostarch
CNWs **:** Cellulose nanowhiskers
DBTDL **:** Dibutyltin dilaureate
DMF **:** Dimethylformamide
DS **:** Degree of Substitution
EDC **:** N-(3-dimethylaminopropyl)-N'-ethylcarbodiimide
EDX **:** Energy dispersive X-ray spectroscopy
FTIR **:** Fourier-transform infrared spectroscopy
GPa **:** Giga Pascal
H2SO4 **:** Sulphuric Acid
IPTS **:** isocyanatepropyltriethoxysilane
MCC **:** Microcrystalline Cellulose
MPa **:** Mega Pascal
NaBr **:** Sodium Bromide
NaClO **:** Sodium Hypochloride
NHS **:** N-hydroxysuccinimide
NMR **:** Nuclear magnetic resonance
P(3HB) **:** Poly (3-hydroxybutyrate)
PBAT **:** Polybutylene adipate terephthalate
PCL **:** Polycaprolactone
PEG **:** Polyethylene Glycol
PGMA **:** Polyglycidyl methacrylate
PLA **:** Polylactide

PLLA **:** Poly(L-Lactide)

PMMA **:** Poly(methyl methacrylate)

PS **:** Polystyrene

rpm **:** revolutions per minute

RT **:** Room temperature

SEM **:** Scanning Electron Microscope

TEM **:** Transmission Electron Microscope

TEMPO **:** 2,2,6,6-tetramethylpiperidine-1-oxyl radical

TPS **:** Thermoplastic Starch

XPS **:** X-ray photoelectron spectroscopy

XRD **:** X-ray powder diffraction

SYMBOLS

^{o}C	: Degree Celcius
2θ	: Diffraction angle
E'	: Storage Modulus
T_g	: Glass Transition Temperature
W	: Weight
T_i	: Initial Thermal Degradation Temperature
T_m	: Temperature at the Maximum Degradation Rate
T_f	: Final Thermal Degradation Temperature
M_l	: Mass Loss
h	: Hour
T_c	: Cold Crystallization Temperature
T_m	: Melting Temperature
ΔH_{cc}	: Cold Crystallization Enthalpy
ΔH_m	: Melting Entalpy
σ	: Tensile Stress
ε	: Strain at Break
T_{onset}	: Temperature at which Degradation Starts
E	: Elastic Modulus
m	: Mass
Xc	: Crystallinity
$t_{1/2}$	: Half Time of Crystallization
G'	: Storage Modulus
tan δ	: loss tangent

LIST OF TABLES

Page

LIST OF FIGURES

Page

SURFACE MODIFIED CELLULOSE NANOCRYSTAL INCORPORATED NANOCOMPOSITES

SUMMARY

Cellulose nanocrystal (CNC) can be a good alternative to be used as a nanofiller in polymer matrix because of its superior properties such as lightweight, high mechanical strength and elastic modulus, high surface area, etc. Also, CNC has abundant sources and biodegradable material. It is obtained from a variety of cellulose sources. Thanks to these properties, eco-friendly nanocomposites can be produced. On the other hand, it includes a significant drawback. Due to their hydrophilic nature, CNC shows agglomeration in the polymer matrix, especially in the hydrophobic polymer matrix. In the literature, successful results were obtained for CNC nanocomposites by using the solution casting method. However, the solution casting method is not suitable for large-scale production and is not environmentally friendly due to using of solvents such as DMF, THF, etc. Compared to the solution casting method, melt mixing is environmentally friendly as no solvent is used in the production steps. Also, this method can give information about large-scale production. Despite these advantages, agglomeration of CNC is a noticeable drawback for CNC nanocomposites which are produced by using the melt mixing method. To eliminate this drawback, CNC can be modified with some chemical structures by using modification methods such as esterification, amidation, and polymer grafting. In this study, the aim is to obtain a new nanofiller with modification of CNC and produce bionanocomposites since a majority of petroleum-based polymers cause non-degradable wastes in the environment. To solve this problem, biodegradable polymers are crucial. These polymers such as Poly (butylene adipate terephthalate) (PBAT) have a significant potential to be used in commodity and biomedical applications, whereas PBAT cannot show sufficient mechanical properties and its mechanical strength and elastic modulus can be improved with some changes in the structure, for instance, the addition of CNC. In this study, CNC was modified with PGMA by using the grafting from method. Before the modification step, neat PGMA was synthesized and added to the PBAT matrix to observe the effects of PGMA on PBAT. In the PGMA modification of CNC, the polymerization reaction took place on the CNC surface and FTIR analysis was performed to determine changes in chemical structure. In FTIR analysis, a peak at 1725 cm-1 which is related to C=O was obtained. Modified CNCs were introduced in the PBAT matrix with 3 wt.%. Following the production step, thermal and rheological analyses were performed to characterize specimens. With thermal analysis, crystallization behavior and thermal properties were determined as well as with rheological analysis, improvement of dispersion was detected. For PBAT/CNC-g-PGMA5, a dramatic increase was obtained.

YÜZEY MODİFİYE SELÜLOZ NANOKRİSTAL KATKILI NANOKOMPOZİTLER

ÖZET

Selüloz nanokristal (CNC), selülozun asit ile hidrolizinden elde edilen bir nano malzemedir. Asit hidrolizi ile birlikte kristalin bölgeler varlığını korurken amorf bölgeler ise parçalanmaktadır. CNC'nin yüksek mekanik mukavemeti, elastik modülünün yanı sıra yüksek yüzey alanına sahip olması gibi önemli avantajları bulunmaktadır. Bu dikkate değer özellikleri sayesinde polimer kompozitler için önemli bir takviye alternatifi olarak görülmektedir. Bu üstün özelliklerinin yanı sıra CNC'nin elde edilmesi için kaynak bolluğunun olması ve biyobazlı olması gibi avantajları bulunmaktadır. Günümüz şartlarında, çevre dostu malzemelere olan önem de git gide artmaktadır. Burada CNC bu değerli özellikleri sayesinde göze çarpmaktadır.

Son yıllarda CNC hakkında yapılan yayınlar ve bu yayınların aldığı atıflarda önemli bir artış söz konusudur. Bununla birlikte polimer matrisleri içinde iyi bir CNC dağılımı elde etmek oldukça zorlu bir işlemdir. CNC yüzeyindeki -OH grupları nedeniyle birbirleriyle hidrojen bağları kurmaktadır. Bu fiziksel etkileşimler nedeniyle de özellikle hidrofobik polimer matrisleri içersinde CNC aglomerasyonları görülmektedir.

CNC'nin polimer matrisleri içersindeki dağılımını geliştirmek için birçok yöntem denenmiş ve bunlarla ilgili çalışmalar yapılmıştır. Bunlardan ilk akla gelen ise çözelti dökümü ile polimer nanokompozitlerin üretilmesidir. Bu yöntemde dimetilsülfoksit (DMSO), tetrahidrofuran (THF), kloroform (CHL), dimetil formamid (DMF) gibi çözeltiler kullanılmaktadır. Bu çalışmalarla birlikte CNC'nin dağılımında olumlu sonuçlar elde edilmiştir. Ancak, çözelti dökümü ile yapılan üretimler laboratuvar ölçekli olup, büyük ölçekli üretimler için yetersiz kalmaktadır. Bu yöntemle ile sadece CNC ve polimer matrisleri arasındaki uyumun arttırılabileceği tespit edilebilmektedir. Bu yöntemin bir diğer dezavantajı ise kullanılan çözeltiler sebebiyle çevre dostu bir üretim şekli olmamasıdır. Bunun için çözelti kullanılmadan laboratuvar ölçekli olarak eriyik karıştırıcı cihazları tercih edilmektedir. Bu cihaz sayesinde, büyük ölçekli üretimler hakkında fikir sahibi olunabilir.

CNC'nin dağılımını geliştirmek için çözelti dökümünün yanı sıra CNC' ye yapılan yüzey modifikasyonlarına başvurulmaktadır. Bu modifikasyonlar fiziksel bağlarla kurulabileceği gibi genellikle esterifikasyon, amidasyon, oksitleme, silanlama ve polimer modiye etme gibi birçok kimyasal yöntemi içermektedir.

Bu tezde de bu yöntemler hakkında bilgi verilmektedir. Bu yöntemler ile modifiye edilmiş selüloz nanokristallerin çözelti dökümü, eriyik proses yöntemleri ile üretilen numunelerin mekanik, termal, reoloji özellikleri ile ilgili literatürde birçok çalışma vardır. CNC'nin yüzeyindeki hidroksil grupları sayesinde kimi zaman ön bir işleme tabi tutulan yüzey ardından bir kimyasal yapı ile modifiye edilmektedir. Örneğin, literatürde de çokca karşılan oksitleme işlemleri bir ön işlem olarak ifade edilmektedir.

Bu işlemin ardından yüzey bazı kimyasal yapılarla, belirli koşullar sağlandığında modifiye edilebilmektedir. Polimer modifikasyonu da sıkça karşılaşılan bir yöntemdir. Bu modifikasyon iki şekilde yapılabilir. Polimer zincirleri direkt yüzeye modifiye edilebilir ya da polimerizayon CNC'nin yüzeyinde gerçekleştirilebilir. İkinci işlem için başlatıcı ve monomer gerekmektedir.

Literatürde bulunan birçok çalışmaya rağmen dikkate değer bir gelişme kaydedilmemiştir. Bu çalışmada CNC ile polimer matrisleri arasındaki etkileşimi arttıracak ve CNC'nin dağılımını geliştirecek bir kimyasal modifikasyon bulunması üzerine durulmuştur. Polimer nanokompozit üretimi için ise biyoparçalanabilir bir malzeme olan Poli (bütilenadipat-ko-tereftalat) seçilmiştir. Bu malzeme biyoparçalanabilir olmasına rağmen mekanik mukavemeti ve elastik modülüsü bakımından gelişime açık bir malzemedir. Bu polimerin mekanik özelliklerinin geliştirilmesiyle birlikte gündelik uygulamalarda ve biyomedikal alanında kullanım alanları geliştirilebilir.

Bu çalışmada CNC yüzeyi PGMA ile modifiye edilmiştir. PGMA seçilirken dikkat edilen iki önemli nokta bulunmaktadır. Bunlardan ilki hidrofobik bir yapıya sahip olmasıdır. CNC'nin hidrofilik doğasından ve kendi arasında oluşturduğu hidrojen bağlarından dolayı aglomerasyon belirgin bir şekilde görülmektedir. Ancak yüzeye modifiye edilen PGMA zincirleri ile birlikte bu hidrofilik karakter azaltılabilir. Ayrıca PGMA zincirlerinin içerdiği epoksi halkaları CNC ile polimer matrisi arasında kimyasal bağ oluşturarak bir köprü oluşturabilir. Proses esnasında epoksi halkaları açılarak polimer matrisi ile kimyasal reaksiyon verebilir. Bu iki nedenden dolayı CNC'nin polimer matrisi içinde dağılımı geliştirilirken, daha iyi özelliklere sahip bir polimer malzeme elde edilebilir. Literatürde PGMA modifikasyonu ile ilgili çalışmalar kısıtlıdır. Bir çalışmada modifikasyon üzerinde durulup, üretilen nanokompozitlerin üzerinde durulmamıştır.

PGMA modifiye edilirken KPS başlatıcısıyla GMA monomeri kullanılmıştır. Polimerizasyon reaksiyonu saf suda gerçekleşmiş olup, polimerizazyon 3 saat boyunca sürmüştür. Polimerizasyon sıcaklığı ise 70 ^{o} C olarak belirlenmiştir. PGMA'in kendi başına PBAT matrisi üzerinde etkisini görmek için modifikasyonsuz halde de sentezleri yapılmıştır. CNC modifikasyonları ve saf PGMA sentezleri için farklı konsantrasyonlarda GMA oranları kullanılmıştır.

Üretilen saf PGMA'ler 0.5,1,5,10 ml'lik GMA'lerin 50 ml'lik saf su içinde polimerleşmesiyle elde edilmiştir. CNC-g-PGMA'ler ise 0.5,1,5 ml'lik GMA'lerin 50 ml saf su içinde 1 gram CNC ile modifiye edilmesi sonucunda sentezlenmiştir. Üretilen modifiye edilmiş CNC'ler santrifüj işleminden geçirildikten sonra kurumaya alınmıştır. Sentezlenen ürünlerin kimyasal yapılarını incelemek için FTIR analizi yapılmıştır. Analiz sayesinde modifiye edilmiş yapılar ile saf CNC arasındaki pik farklılıkları gözlemlenmiştir. Özellikle 1725 cm^{-1} 'de C=O ile ilgili olan pik göze çarpmaktadır. Bununlar birlikte modifiye edilmiş CNC'lere TGA testi yapılmış ve ağırlık kayıpları ile ilgili kıyaslama yapılmıştır.

Modifiye edilmiş ve edilmemiş CNC'lerin yanı sıra sentezlenen saf PGMA'ler ağırlıkça %3 oranında kullanılarak, PBAT matrisi ile karıltırılmıştır. Bu üretim aşaması 160 ^{o}C'de 100 rpm vida hızı ve 5 dakika proses süresi olarak gerçekleştirilmiştir.

Çıkan ürünlerden pres işlemi ile birlikte reoloji diskleri hazırlanmıştır. Reoloji disklerinden CNC-g-PGMA0.5 içeren PBAT'de kahverengi noktalar dikkat çekmektedir. Bu noktalar, proses sıcaklığı ile birlikte modifiye edilmiş CNC'lerin

degradasyonuna işarettir. Az PGMA miktarı ile birlikte yeterince uzun zincirler elde edilememiş ve kısa zincirler proses sıcaklığın etkisiyle bozunmuş olabilir. Bununla birlikte reoloji sonuçları incelendiğinde PBAT/PGMA'lerin reoloji özelliklerinde belirgin bir artış göze çarpmaktadır. PGMA0.5 dışında polimerizasyon için gereken GMA miktarı azaldıkça reolojik özelliklerde artış olduğu gözlemlenmiştir. Bununla birlikte CNC-g-PGMA'lerin PBAT matrisine etkisi incelendiğinde ise en iyi sonuç CNC-g-PGMA 5 için elde edilmiştir.

Reoloji özellikleri nanokompozitlerde takviye malzemenin dağılımındaki gelişime bağlı olarak artış göstermektedir. Özellikle frekans tarama yapılan reoloji analizlerinde düşük frekanslarda elde edilen kompleks viskozite ve depolama modüllerindeki artışlar malzemenin matris içinde dağılımı ile ilgili önemli bilgiler vermektedir.

Numunlerin ayrıca DSC analizleri yapılmış ve modifiye edilen zincirin uzunluğu arttıkça kristalizayon kinetiğine olumsuz etkisi gözlemlenmiştir.

1. INTRODUCTION

Environmental pollution and global warming are the worrying problems of today. Finding new solutions to these problems occupies a significant place in the industry and academy. Cellulose nanocrystal has some advantages to reduce these problems. CNC is extracted from cellulose which is the most bio-based polymer. In addition to being bio-based materials, it has superior mechanical properties, lightweight, low toxicity, and high surface area. These superior features can enable CNC to be used as a reinforcement in polymer matrices especially in biodegradable polymers to obtain eco-friendly composites [1].

In the last years, the interest in CNC increased thanks to its superior properties. As seen in Figure 1.1, publications and citations increased dramatically [1].

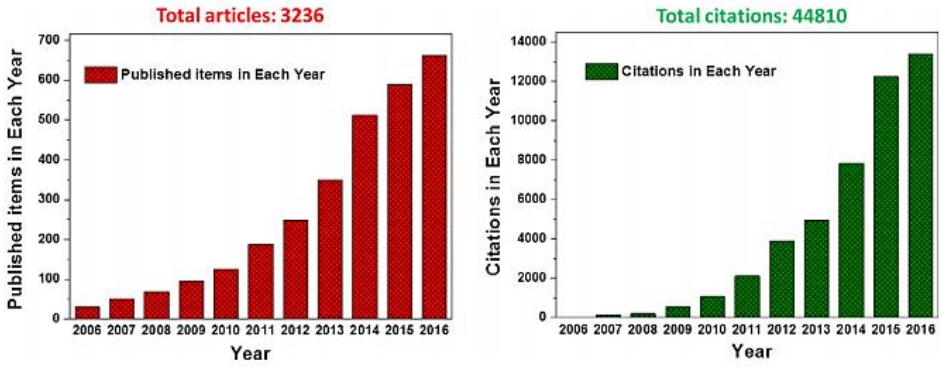

Figure 1.1: Publications and citations about cellulose nanocrystal between 2006 and 2016 [1].

CNC shows hydrophilic character due to hydroxyl groups on its surface as seen in Figure 1.2 and these cause agglomeration of CNCs in hydrophobic polymer matrix.

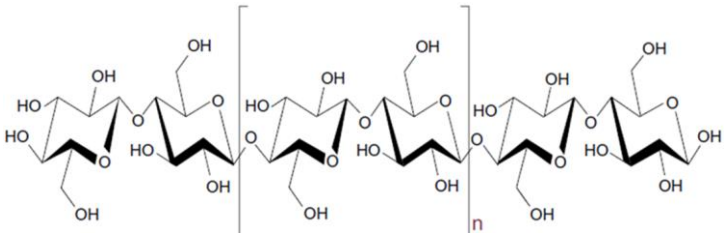

Figure 1.2: Cellulose nanocrystal chemical structure [2].

A significant improvement was observed in CNC nanocomposites which were produced with the solution casting method. However, the solution casting method is not suitable for large-scale production and is not environmentally friendly due to using of solvents. To eliminate this drawback, modification methods can be an alternative. CNC surface can be modified thanks to its hydroxyl groups. Esterification, etherification, silylation, sulfonation, and oxidation are some chemical modification methods for CNC as seen in Figure 1.3 [3].

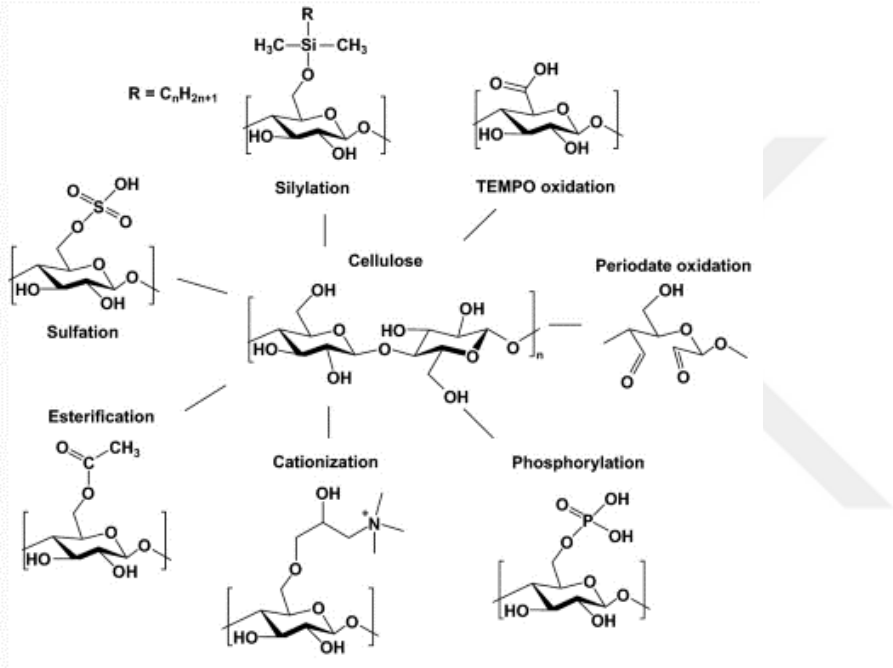

Figure 1.3: CNC chemical modification methods [3].

In addition, polymer grafting is another method and it is divided into two main groups which are grafting onto and grafting from [4].

Although there are numerous methods, a significant improvement was not observed in the literature. In this study, polyglycidyl methacrylate (PGMA) modification took place on the CNC surface with the grafting from method, and PBAT/CNC-g-PGMA nanocomposites were produced by melt mixing. With the addition of modified CNC, rheological and thermal properties were investigated to understand the effects of CNC on the polymer matrix. Also, like cellulose, polybutylene adipate terephthalate (PBAT) is a biodegradable polymer and this contributes to producing an eco-friendly material. PGMA was chosen for modification of CNC due to two main reasons. PGMA is a hydrophobic polymer and epoxy rings can give chemical reactions with polyester such

as polylactide (PLA) and PBAT and consequently, it can contribute to better dispersion in the polymer matrix. In the literature, studies about PGMA modification are insufficient and quite limited. Le Gars et al. [5] studied PGMA modification on CNC surface with atom transfer radical polymerization. PLA/CNC specimens were produced with solvent casting and only SEM analysis was performed to understand the dispersion development. However, it was unsufficient to conduct SEM analysis only to understand the dispersion. In this study, rheological analysis were performed to understand changes in dispersion. Also, nanocomposites were produced by using melt mixing method. Therefore, compared to the study conducted by Le Gars et al., this study is more environmentally friendly and applicable to industrial production.

2. CELLULOSE NANOCRYSTAL (CNC)

Cellulose nanocrystals (CNCs) which consist of cellulose main chains are rod-like crystalline nanoparticles [1]. CNCs are extracted from natural sources such as algae, animals, bacteria, wood, plants etc as shown in Figure 2.1. Tunicates are animal sources to obtain cellulose. Also, cellulose can be obtained from algae which have cell wall. Bacteria are known as another source to produce cellulose nanocrystal. These bacteria produce gel that includes microfibrils and water. Properties of bacterial cellulose nanocrystal depends on culturing conditions [6].

Figure 2.1: Various sources for CNC [6].

2.1 Acid Hydrolysis of Cellulose

Cellulose includes two main structures that are ordered and disordered regions. Ordered regions are also named as crystalline region and disordered regions are amorphous. In acid hydrolysis, strong acids such as sulphuric acid and hydrochloric acids are used to obtain crystalline structures. Kinetics of hydrolysis is vital phenomena to understand the extraction of CNC. In the amorphous region, faster hydrolysis kinetics are observed compared to the crystalline region and consequently, the crystalline regions remain whereas, the amorphous regions are removed as seen in Figure 2.2.

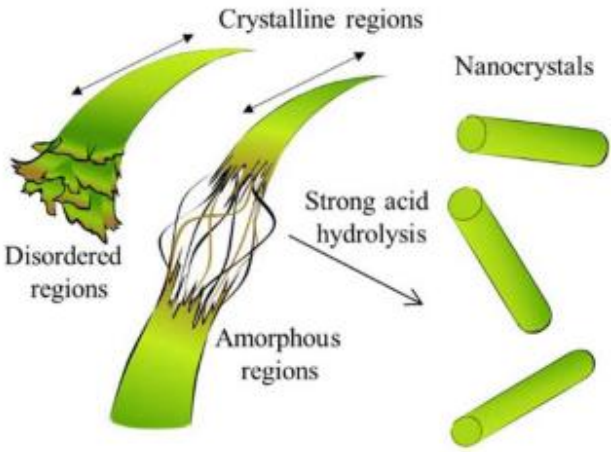

Figure 2.2: Acid hydrolysis of cellulose [7].

In addition to acid hydrolysis, some mechanical treatments can be applied to obtain cellulose nanocrystal. Cryo crushing, microfluidization, and high intensity ultrasonic treatments are some examples of mechanical processes. Although more uniform, and smaller particles can be obtained with mechanical treatments, crystalline structures get some damage and thus, the amount of crystallinity decreases [7].

2.2 Properties of Cellulose Nanocrystal

In addition to being eco-friendly, CNC has some unique properties to use in different applications. These properties can be investigated under four headings that are mechanical, thermal, rheological, and optical properties.

2.2.1 Physical properties of CNC

CNC that has a rod-like shape involves two geometrical dimensions that are length and width. These dimensions depend on cellulose sources and hydrolysis conditions such as acid type, temperature and time. The width of the CNC can be varied from 3 to 50 nm, while values of several micrometers can be obtained for the length of the CNC [2].

The spect ratio has a crucial role in obtaining high mechanical properties in the polymer matrices. It is calculated by the L/D ratio. L is the length of CNC and D is the diameter of CNC. Increasing the L/D ratio contributes to improving the network

formation in the polymer matrices and consequently, the mechanical properties of the polymer can be increased dramatically [2].

2.2.2 Chemical properties of CNC

Cellulose nanocrystals include cellulose main chains and these chains consist of repeating dimer units that are cellobiose as shown in Figure 2.3. On the contrary of disordered cellulose chains, CNC is less reactive because the acid can not spread into the structure easily due to the ordered structure.

Cellulose nanocrystal has hydroxyl groups on their surface. These groups can give reactions with numerous chemical structures and surface chemistry can be tailored with acid type in the hydrolysis step. For instance, sulfate groups can be obtained by H_2SO_4 hydrolysis. Also, aldehyde, amino, and thiol groups can be obtained with mild-post hydrolysis reactions [8].

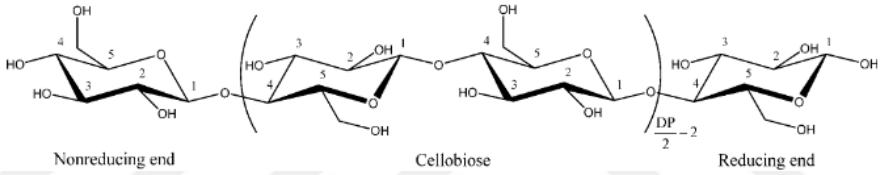

Figure 2.3: Chemical structure of cellulose [8].

2.2.3 Mechanical properties of CNC

The mechanical properties of CNCs depend on some parameters that are anisotropy, nanocrystal defects and crystalline amount. Atomic force microscopy (AFM), X-Ray diffraction analysis, and Raman spectroscopy can be used to determine the mechanical properties of CNC. CNC shows desirable mechanical properties such as high elastic modulus (100-140 GPa) and tensile strength (7500 MPa) [1].

2.2.4 Thermal properties of CNC

The thermal degradation temperature of CNC is crucial to understanding its potential applications. The degradation or decomposition temperature range is between 200 ^oC to 300 ^oC for CNC. It depends on sources, isolation, processing method, heating rate and surface modifications are some critical parameters that affect the thermal degradation of CNCs. Also, the number of sulfate groups on the CNC surface affects the thermal stability of CNC and desulfation treatment enables to obtain thermal stability [7].

Petersson et al.[9] studied on the degradation of Cellulose nanowhiskers (CNWs). In this study, they focused on three different nanowhiskers that are butanol cellulose nanowhisker (BCNW) and surfactant cellulose nanowhisker (SCNW). Thermal analysis was performed and degradation of these whiskers was compared.

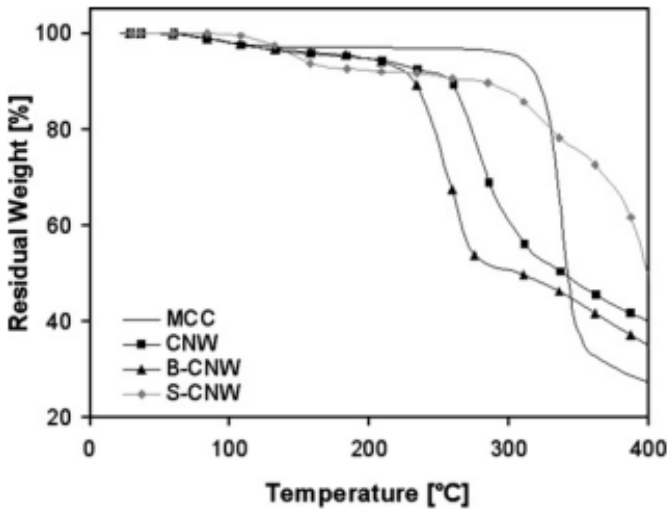

Figure 2.4: Thermogravimetric analysis of microcrystalline cellulose (MCC) and nanowhiskers [9].

Below 150 ^{o} C a slight weight decrease was observed for all cellulose nanowhiskers because of the release of moisture from the structure. The onset degradation temperature is the temperature at which the degradation starts. The onset degradation temperature is lower for CNW and BCNW than MCC as given in Figure 2.4. This was explained by the acid hydrolysis effect on thermal stability. More steps are applied to obtain nano cellulosic materials [9].

3. SURFACE MODIFICATION METHODS AND THEIR USE FOR VARIOUS APPLICATIONS

3.1 Esterification

Esterification reaction takes place between carboxylic acids and alcohols. As a result of this reaction, ester and water are obtained as products. Also, ester products can be obtained with the reaction between acyl chloride and alcohol [10].

Hydroxyl groups that are on the surface of cellulose nanocrystal can react with carboxylic acids and change the chemical structure of cellulose nanocrystal. In the literature, it was found that CNC modification by using the esterification method decreases hydrophilicity and agglomeration in non-polar polymer matrices. In one study, Lauroyl chloride was modified on cellulose nanocrystal surface with esterification method in the presence of pyridine catalyst as given in Figure 3.1. In this study, the effects of CNC and modified CNCs on the properties of epoxy composites were investigated [11].

3 different cellulose nanocrystal were obtained with surface modification because of different degree of substitution values. The degree of substitution increased with the increase of catalyst and monomers [11].

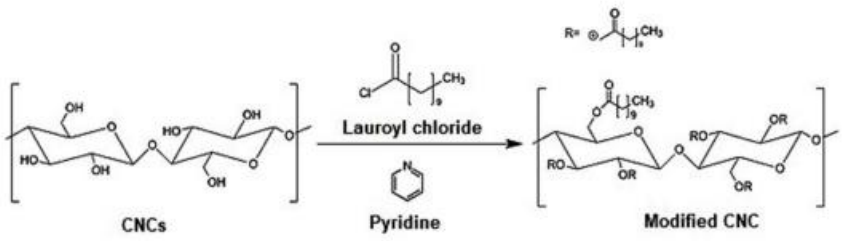

Figure 3.1: CNC modification with lauroyl chloride [11].

In FTIR analysis, peaks at 1750 cm^{-1} which is related to carbonyl were obtained. In XRD analysis, neat CNC gives three peaks and one of them is broad. Lauryl chloride modified CNCs have a different peak from neat CNC. This peak was observed at 2θ of 20 ^{o} [11].

As seen in Figure 3.2, modified CNCs that have a degree of substitution of 0.2 and 0.8 showed 3 main peaks. However, CNC with DS of 2.4 showed weak crystallinity and the peak was stronger at 2θ of 20^{o} due to the crystallization behavior of lauryl chloride chains [11].

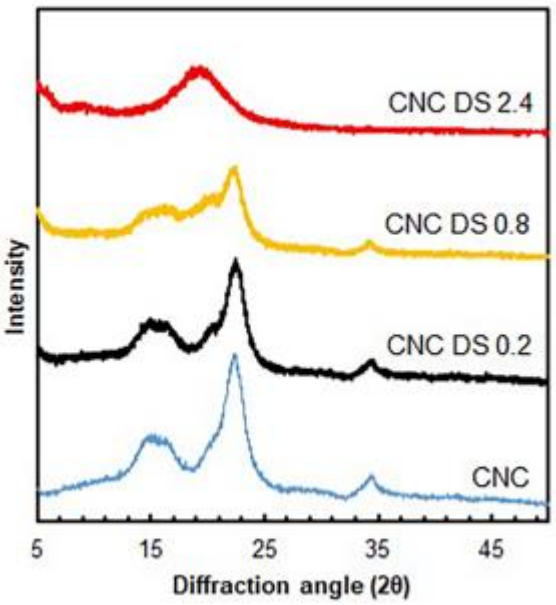

Figure 3.2: XRD analysis of neat and modified CNCs [11].

Contact angle measurements are performed to give information about wetting properties of materials. In this study, contact angle measurements were conducted to understand surface properties of cellulose nanocrystals. As expected, neat CNC has the lowest contact angle due to its hydrophilic nature. The contact angle increased with increasing degree of substitution. Because, hydroxyl groups are decreased with increasing length of hydrophobic chains on CNC surface. The contact angle became 74^{o} with DS of 2.4 [11].

Also , thermogravimetric analysis (TGA) were conducted and they observed improvement of thermal stability with surface modification. Especially, the improvement in thermal stability is evident for modified CNC (D.S 2.4) [11].

In this study, epoxy nanocomposites were produced with modified and unmodified cellulose nanocrystals at different weight ratios that 2.5 % and 5%. Tensile test was applied to epoxy nanocomposites. Contrary to CNC (D.S 0.2) and CNC (D.S 0.8), CNC (D.S 2.4) has a negative effect on the tensile strength of nanocomposite. This was explained by the damage to the crystalline structure. Also, the highest elongation

at break value was obtained with CNC (D.S 2.4) because of the plasticization effect of aliphatic chains. As a result of dynamic mechanical analysis, epoxy has the lowest storage modulus. This situation was explained by the restriction of chain movement with cellulose nanocrystals [11].

In another study, an esterification reaction takes place in the presence of citric acid catalyst. Acetic anhydride was used as a reagent and reaction medium in the acetylation of CNC reaction. They obtained acetylated CNC with a single step and non-toxic catalyst [12].

Acetylation of CNC took place by using two different catalyst amounts that are 0.0052 mmol/mL or 0.052 mmol/mL under 120 ^{o} C for 3 hours. Depending on catalyst amount, they obtained two different degrees of substitution (0.18 and 0.34) [12].

Neat and acetylated CNC suspensions were prepared with water and chloroform in order to determine the change in hydrophilicity. While neat CNC-water is a stable suspension, neat CNC precipitated in chloroform quickly. On the other hand, acetylated CNC is more stable in chloroform compared to neat CNC. Precipitation of acetylated CNC in chloroform occurred slower and in a lower amount. This indicates that hydrophilic character is decreased by the esterification of CNC [12].

Citric acid did not give considerable a reaction with cellulose nanocrystal. This was explained by NMR analysis of acetylated CNC. They did not observe any resonances at 44 ppm that correspond to methylene groups of citric acid. [12]

Spinella et al. [13] prepared PLA/CNC nanocomposites with lactide and acetate modification by extrusion. In this study, they aimed to increase the thermal properties of PLA. CNCs were synthesized from cotton linter. Lactide and acetate were grafted on CNC surface with esterification. A new peak was observed at 1736 cm $^{-1}$ for lactide and acetate modified CNCs (CNC-lactide and CNC-g-acetic acid). Also, neat CNC and modified CNCs have the same peak at 1162 cm $^{-1}$ showing vibrational stretches of C-O-C. Spinelle et al. [13] calculated the degree of substitution for modified CNCs by proportioning the intensities of the peaks at 1162 cm $^{-1}$ and 1736 cm $^{-1}$.

PLA/ CNC nanocomposites were produced at 30 rpm for 3 minutes and afterward at 60 rpm for 5 minutes under 120 ^{o} C. And then, specimens were prepared by injection molding. In injection molding, mold temperature was 50 ^{o} C and oven temperature was 200 ^{o} C. Lastly, the anneling of specimens took place at 130 ^{o} C for 1 h [13].

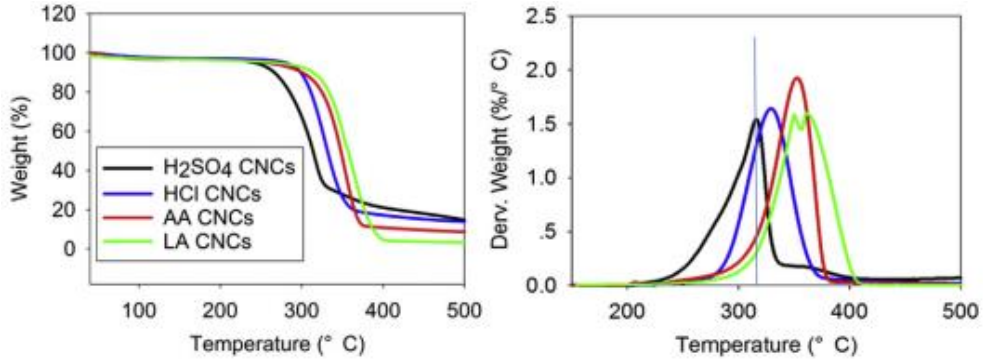

Figure 3.3: Thermogravimetric analysis of modified CNCs [13].

Thermogravimetric analysis was performed under nitrogen environment. CNCs obtained from H_2SO_4 hydrolyzed showed the worst thermal stability in modified CNCs. Thermal stability increased by modification of CNC and CNC-Lactide showed the best thermal stability as seen in Figure 3.3 [13].

Also, Spinelle et al. [13] conducted a dynamic mechanical analysis. Storage modulus was determined under different temperatures. In Figure 3.4, 5% of modified and unmodified CNCs were included in nanocomposites and they showed different storage modulus values under the different temperatures. PLA/CNC-LA has the highest storage modulus below and above its Tg.

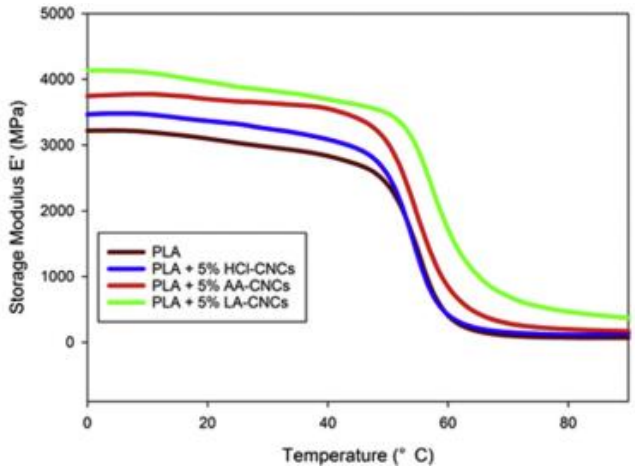

Figure 3.4: Storage modulus of PLA and nanocomposites [13].

They also investigated heat deflection temperatures of PLA and PLA/CNC-LA nanocomposites. Heat deflection temperature was increased by the addition of CNC-LA as seen in Figure 3.5 [13].

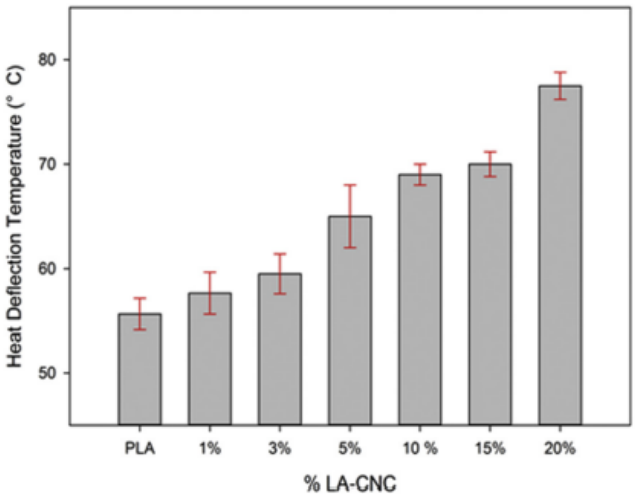

Figure 3.5: Heat deflection temperature of PLA and its nanocomposites with CNC-LA [13].

3.2 Transesterification

Wei et al [14] obtained transesterified CNC with a transesterification reaction. Transesterification is a reaction that enables conversion from triglycerides to alkylesters. Triglicerides and alcohols are reagents in transeterification. Methanol and ethanol are generally used because they are both inexpensive and easily accessible [15].

Wei et al [14] modified CNC with canola oil fatty acid methyl ester (CME). CME was synthesized from canola oil that is a vegetable oil. Vegetable oils include three fatty acid chains and these chains are bonded with only one glycerol molecule [16].

In this study, the reaction mechanism consists of two steps. The first step occurred by reaction of triester of glycerol and methanol at 70 ^{o}C. The second step was CME grafting on the CNC surface by using K_2CO_3 catalyst and obtaining CNC fatty acid methyl ester (CNCFE) [14].

The modification took place under two temperatures (100 ^{o}C and 120 ^{o}C) and for various times (4,8,14,20 and 30 h). After each modification, weight percentage gain (WPG) was calculated by the following formula [14]:

$$WPG\% = ((W_{CNCFE} - W_{CNC})/W_{CNC}) \times 100 \quad (3.1)$$

W_{CNCFE} is the weight of modified CNC after vacuum drying. Also, W_{CNC} is the weight of unmodified CNC. WPG% generally increases with reaction time. However, any

increment was not observed from 20 to 30 hours. Also, WPG% has a raise with increasing reaction temperature; however, they observed darkening of CNC. This discoloration may occur with the degradation of CNCs under high temperatures. In this study, the transesterification reaction occurred successfully as the FTIR result implies. Also, it has been proved by XRD analysis that the crystalline structure was not damaged. As well as, the water contact angle was measured to determine the hydrophilicity changes. The variation of dynamic water contact angle with time is shown in Figure 3.6 Water contact angle was increased by transesterification of CNC (62^{o})[14].

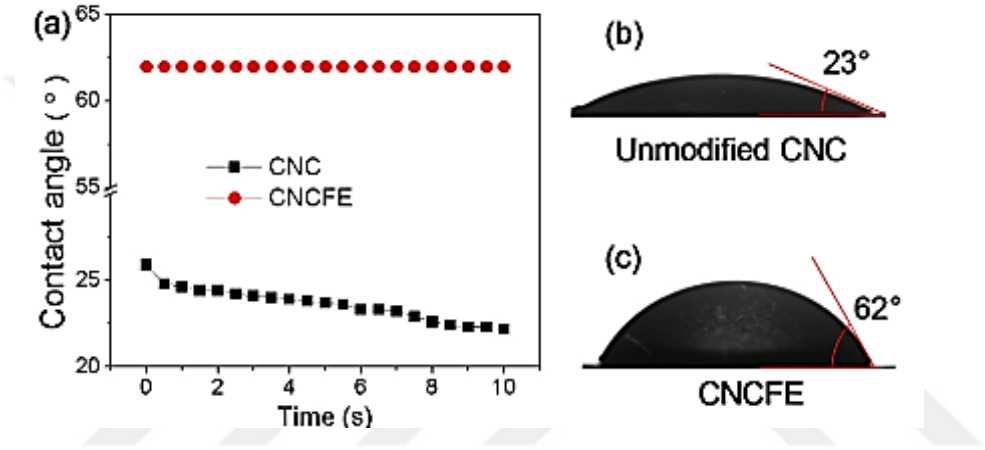

Figure 3.6: a)Contact angle measurement during time contact angle images for b)unmodified CNC and c) CNCFE [14].

3.3 Silylation

Silylation is another chemical modification method to obtain modified CNC. With the silylation method, small molecules can be grafted on CNC surface. Khanjanzadeh et al. [1] used 3-aminopropyltriethoxysilane (APTES) to silylation of CNC. The chemical structure of APTES is shown in Figure 3.7 [17].

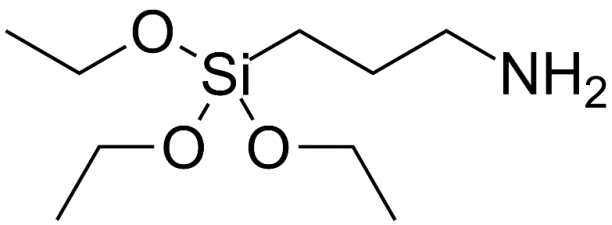

Figure 3.7: Chemical structure of 3-aminopropyltriethoxysilane (APTES) [17].

In this study, it is aimed to increase the use of cellulose nanocrystals in hydrophobic polymer matrices and to create a usage area as a nano adsorbent. Silylation or silane grafting includes three steps that are shown in Figure 3.8. Firstly, hydrolysis of the silane takes place and silanol is formed. After that, silanols and CNCs form hydrogen bonding. Lastly, the Si-O-C bond is formed. No hazardous solvents was used during the syntesize of modified CNC [17].

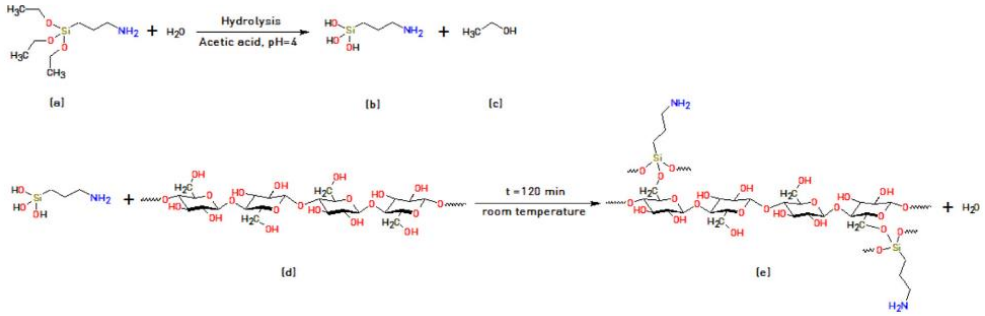

Figure 3.8: a) APTES b) Silanol c) Ethanol d) CNC e) Silane grafting CNC [17].

Khanjanzadeh et al. used Attenuated total reflection infrared spectroscopy (ATR-IR) to understand if the modification was successful. They observed a new band at 1550 cm^{-1} a shown in Figure 3.9. As well as, Si-O-C bonds have a specific band of about 1135 cm^{-1}, 1150 cm^{-1} . These peaks cannot be observed easily. Because vibration bands of C-O-C are in the same region [17].

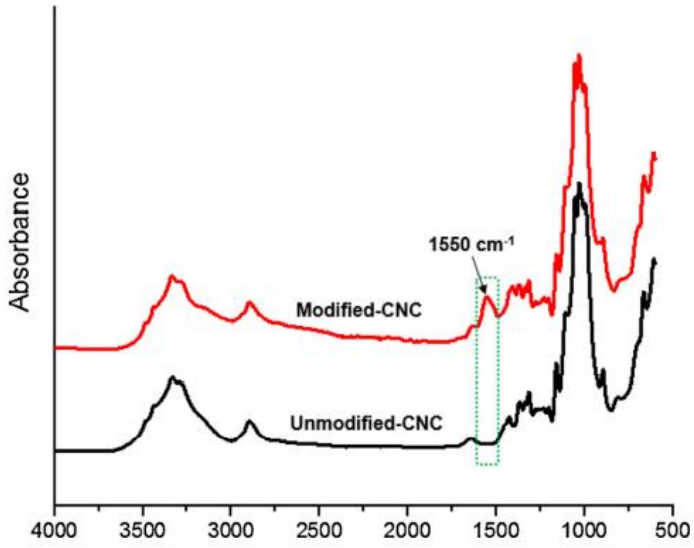

Figure 3.9: ATR-IR analysis of modified and unmodified CNCs [17].

Also, energy dispersive x-ray spectroscopy (EDX) was used to determine the existence of APTES in the product of the modification reaction. Unlike CNC, APTES contains silicon (Si) and nitrogen (N) elements. EDX spectrum of modified CNC has peaks of Si and N as seen in Figure 3.10 [17].

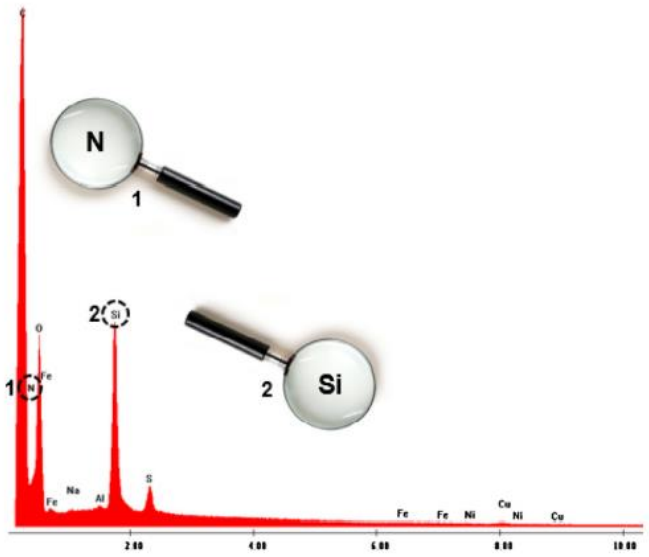

Figure 3.10: EDX spectrum of modified CNC [17].

TGA was conducted under nitrogen environment and the degredation behavior of CNC and APTES modified CNC were determined. An increase with modification of CNC by 10 ^{o}C was seen in initial thermal degradation temperature (T_i). Tm (tthe temperature at the maximum degradation rate) and T_f (final thermal degradation temperature) also increased as seen in Table 3.1 [17].

Table 3.1: TGA and DTG data of unmodified and modified CNC under nitrogen at 10 ^{o}C min^{-1} [17].

Parameters	**Unmodified CNC**	**Modified CNC**
T_i	258	268
T_f	322	341
T_m	284	293
%M_l (150^{o}C-350 ^{o}C)	54.7	49.4
%M_l (25 ^{o}C -500 ^{o}C)	71.7	65.9
% Residual Mass at 500 ^{o}C	28.3	34.1

In addition to increasing the thermal properties of CNC, this method ia a simple method to obtain modified CNC. Also, modified CNC will be an option for nano adsorber thanks to amino groups on its surface [17].

3.4 TEMPO (2,2,6,6-tetramethylpiperidine-1-oxyl radical) Mediated Oxidation

Primary alcohol groups can be converted to carboxylic acid groups in TEMPO mediated oxidation and oxidized CNC is obtained. This modification method involves NaBr, NaClO and TEMPO chemicals. Hydroxyl groups on the CNC surface decreased by TEMPO mediated oxidation [4]. Tempo mediated oxidation is also pretreatment to modify long or small chains on the CNC surface. For example, Le Gars et. al [18] conducted amidation reaction on oxidized CNC surface. In another study, They studied PEG adsorption on oxidized CNC [19].

TEMPO mediated oxidation steps are given in Figure 3.11. Formation of hypobromite ion (BrO^-) is the first step and nitrosonium salt is formed in the second step. Primary alcohol groups are oxidized in the third step [20].

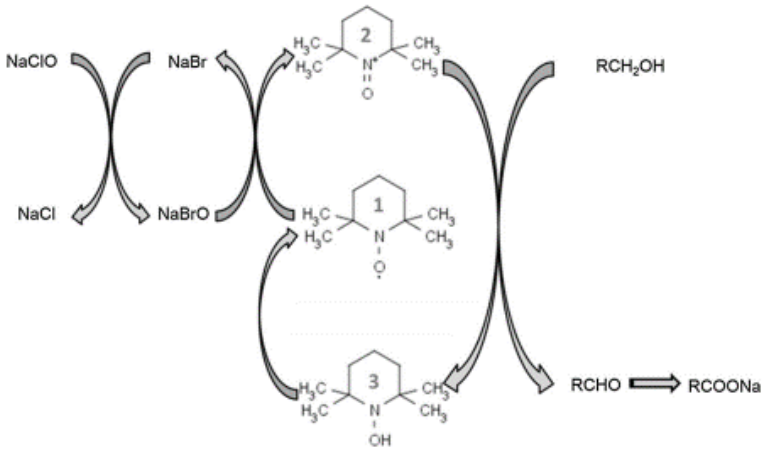

Figure 3.11: Reaction mechanism of TEMPO mediated oxidation [20].

Fraschini et al. [20] investigated the effects of various parameters in TEMPO mediated oxidation. Firstly, the effects of reaction temperature on reaction kinetics are seen in Figure 3.12. They chose two different temperatures (4 °C and 25 °C) and the amount of the acid content was determined with reaction time. At 25 °C, the plateau that 1500 mmol kg^{-1} was obtained in the first 10 minutes. The total acid content was obtained by conductometric titration.

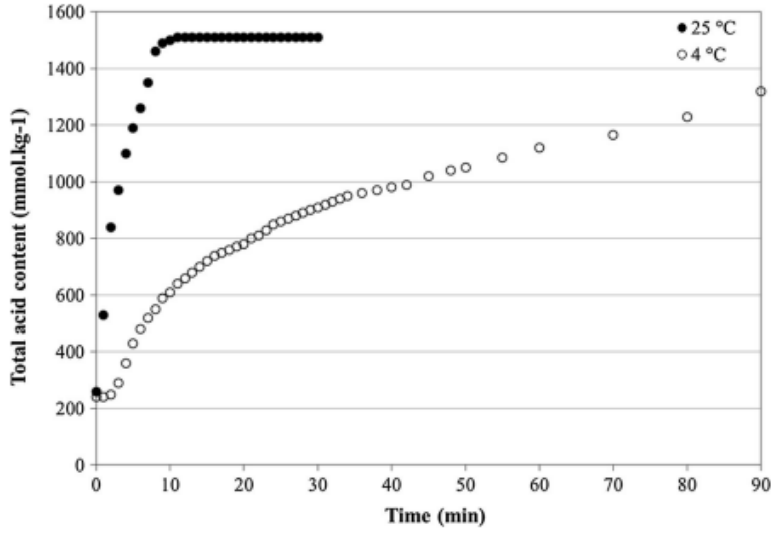

Figure 3.12: Effects of reaction temperature on total acid content at different times [20].

Also, they investigated the effects of NaClO amount on total acid content. It can be seen in Figure 3.13. After 0.4 mol/ mol ofprimary alcohol, they observed a plateau at 4 ^{o} C. On the other hand, total acid content constantly increased with the addition of NaClO. No plateau was observed due to damage in cellulose nanocrystal structure [20].

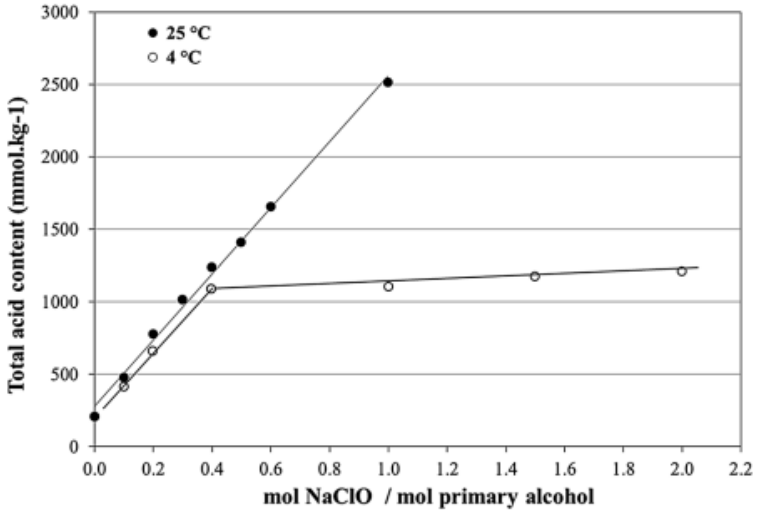

Figure 3.13: Effects of amount of NaClO on total acid content at different temperatures [20].

3.5 Amidation

Amine groups can not give reaction with hydroxyl groups on CNC surface. Amidation could take place with oxidized CNC. Because, unlike hydroxyl groups, carbonyl groups can give reaction with amine groups. Ammonia involves one nitrogen and three hydrogen elements. As seen in Figure 3.14, amines are obtained to replace of one or more hydrogen atoms with alkyl or aryl groups [10].

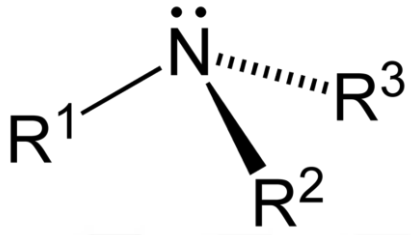

Figure 3.14: Chemical structure of amine [10].

According to hydrogen amount, amines are divided into three groups that primary, secondary and tertiary amines. As seen Figure 3.15, unlike amine, amide include carbonyl groups [10].

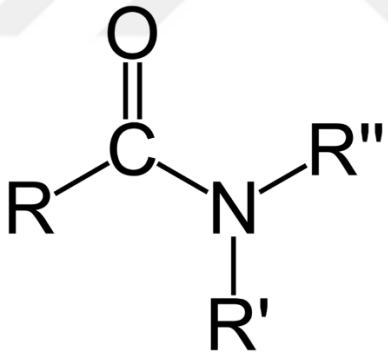

Figure 3.15: Chemical structure of amide [10]

Le Gars et al. Performed a modification of 1-methyl-3- phenylpropylamine on the CNC surface. N-(3-dimethylaminopropyl)-N'-ethylcarbodiimide (EDC) and N-hydroxysuccinimide (NHS) were used as the catalysts. Amidation reactions took place for different reaction times (24,48, 72 h.). To characterization of modified CNCs, FTIR analysis was performed under the acid and base conditions [18].

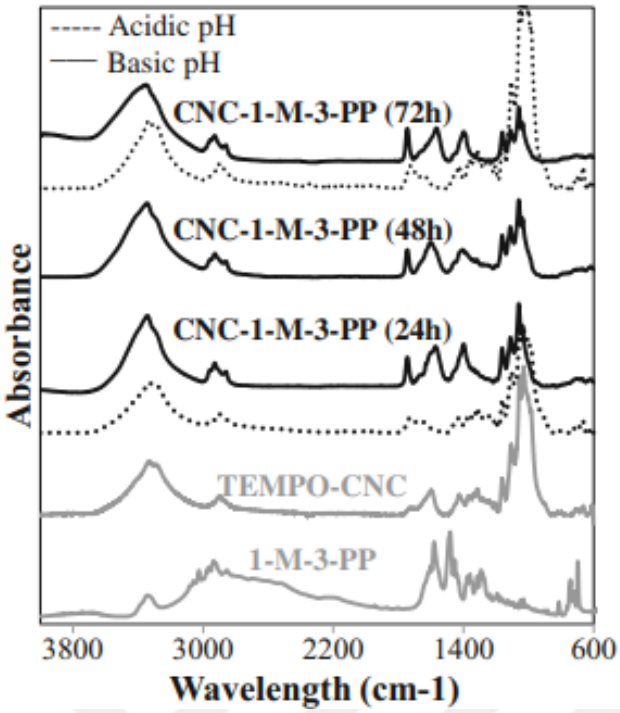

Figure 3.16: FTIR analyis of various of CNC-1-M-3-PP, TEMPO-CNC and 1-M-3-PP [18].

For CNC-1-M-3-PP, the peak at 1650 cm^{-1} that shows the presence of –N(H)–C=O was observed under acidic conditions. As seen in Figure 3.16, this peak was observed at 1745 cm^{-1} under base conditions [18].

Also, Chen et al. [21] studied on amidation of freeze dried CNC surface with chitosan. Chitosan includes amine groups on its surface. Before the amidation step, CNCs crosslinked with citric acid at 110 ^{o}C for 4 h. Amidation took place at room temperature for 6 h. Modification steps can be seen in Figure 3.17.

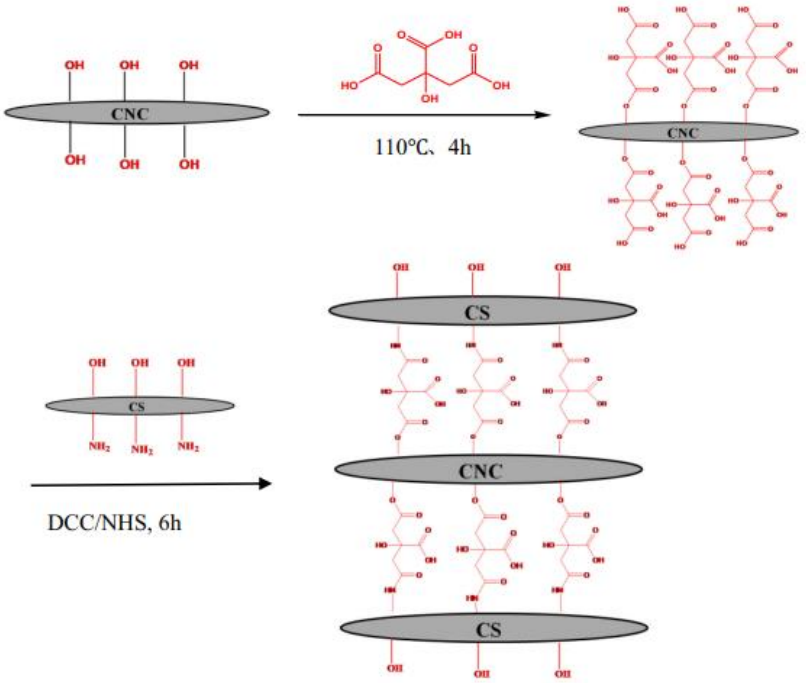

Figure 3.17: Chitosan modified on crosslinked CNCs by amidation[21].

In this study, they aimed to obtain successful modification and to use it as a filler in corn nanostarch (CNS). CNC, CNS, and glycerol were used to prepare nanocomposites with solution casting. Glycerol was used as a plasticizer. The success of the modification was determined by XPS and FTIR analysis. Also, they focused on the antibacterial activities of CNS nanocomposites. For this property, they investigated inhibition zones of nanocomposites and pure CNS with using E.coli and S.aureus as seen in Table 3.2 [21].

Table 3.2: Inhibition zone (mm) measured for antibacterial activities [21].

Sample	Inhibition zone (mm)	
	E. coli	S. aureus
Pure CNS film	0	0
CNS/modified-CNCs: 2.0wt%	12.35±0.85	14.46±0.98
CNS/modified-CNCs: 4.0wt%	15.27±0.96	17.51±1.08
CNS/modified-CNCs: 6.0wt%	18.76±1.17	20.10±1.21
CNS/modified-CNCs: 8.0wt%	22.24±1.25	23.96±1.32
CNS/modified-CNCs: 10.0wt%	22.47±1.27	23.85±1.31

The inhibition zone increased by increasing the amount of modified CNC. This situation was explained by the positive effects of amino groups [21].

3.6 Urethanization

In urethanization, urethane bonds are obtained by the chemical reaction between hydroxyl groups and isocynate such as isocyanatepropyltriethoxysilane (IPTS), n-octadecyl isocyanate ($C_{18}H_{37}NCO$) [22,23,24]. Urethanization is also called as carbanylation [4].

Taipina et al. [22] studied on IPTS modification of CNC surface and conducted FTIR, (CP-MAS NMR) of 29Si, XRD analysis of modified CNC. As seen in Figure 3.18, IPTS modified on CNC and oligomeric polysilsesquioxane structure was obtained.

1 gram of CNC was suspended in 250 ml of DMF under the nitrogen environment. Then, a trace amount of IPTS was added to the solution and stirred for 8 h. After 8 hours, dibutyltin dilaureate (DBTDL) was added in the mixture with water.

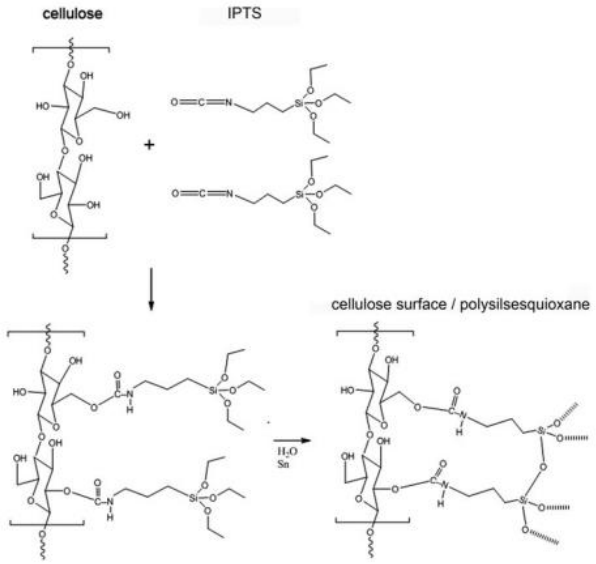

Figure 3.18: Modification of CNC with IPTS [22].

In another study, chemical modification of n-octadecyl isocyanate ($C_{18}H_{37}NCO$) on the CNC surface took place by the urethanization method. Also, they used modified CNC as a nanofiller in the PCL matrix and compare the mechanical and thermal properties of prepared nanocomposites. Unmodified CNC(UMW) and modified CNC was added to PCL matrix with different amounts (3, 6, 9, and 12 wt.%) [23].

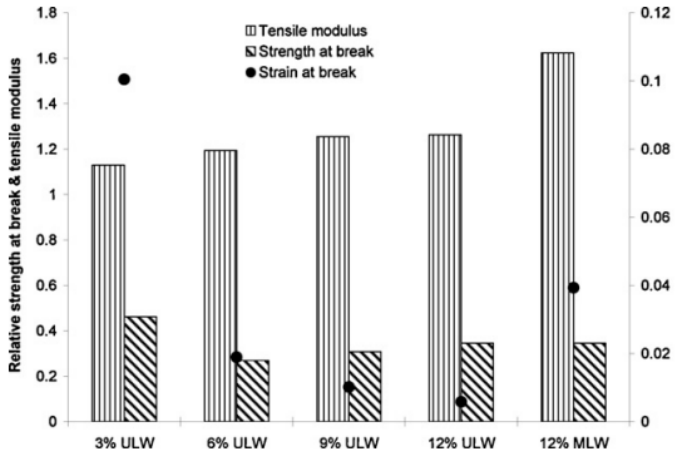

Figure 3.19: Mechanical test results of PCL nanocomposites [23].

Tensile modulus was increased slightly by increasing the amount of CNC content in the PCL matrix. Also, strain at break was decreased in the same situation. On the other hand, compared to unmodified 12 wt.% ULW, 12 wt.% MLW showed higher tensile modulus and strain at break. The degree of crystallinity was calculated thanks to DSC analysis. For the same amount of nanofiller that is 12 wt.%, the degree of crystallinity increased from 0.51 to 0.64 [23].

3.7 Polymer Grafting

As seen in Figure 3.20, this method is divided into two groups that are grafting to or onto and grafting from. In the grafting onto method, the polymer that is grafted on the CNC surface is synthesized before the grafting step. The polymer branches are characterized before the modification in the grafting onto method.

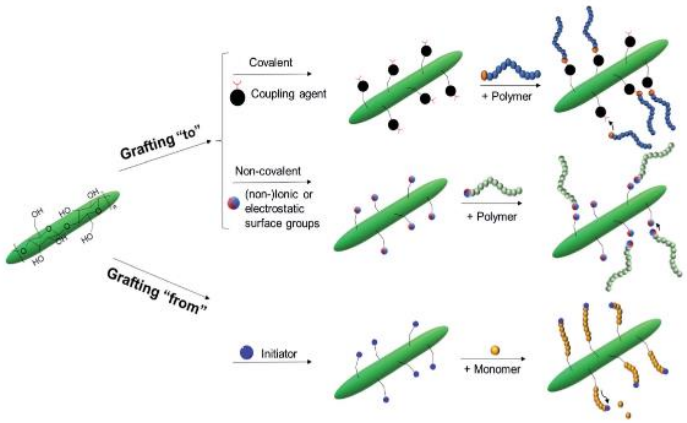

Figure 3.20: Polymer grafting methods [25].

Also, it contributes to controlling the properties of modified CNC. Despite some advantages, grafting density is a huge problem in the grafting onto method due to steric hindrance [4].

Although the characterization of polymer brushes is difficult, a higher grafting density is obtained by grafting from method. In this method, the polymerization reaction takes place on the CNC surface [4].

3.7.1 Grafting onto

Tang et al. studied the grafting onto method with NH_2 terminated polystyrene (PS) in order to obtain amphiphilic nanoparticles. These systems can be found using areas such as biomedicine, pharmaceuticals, and cosmetics [26].

Figure 3.21: Grafting of PS on CNC surface [26].

In this study, 0.5 g CNC and 50 mg amine terminated polystyrene gave reaction in the presence of 5 mg of sodium cyanoborohydride under the nitrogen environment at rt. and 70 ^{o}C [26].

Zhang et al. studied PEG grafted on the CNC surface with the grafting onto method. PLA nanocomposites were prepared with PEG grafted CNC (CNC-g-PEG). Their aim was to obtain nanofibers for bone tissue engineering. In this study, epoxy terminated PEG was synthesized from hydroxyl terminated PEG (PEG-OH). After that, the modification step was carried out at 65 ^{o}C for 6.5 hours. Before the electrospinning process, PLA/CNC-g-PEG nanocomposites were prepared by the solution casting method [27].

They conducted some tests to analyze nanofiller and nanocomposites. To get information about the chemical structure of CNC-g-PEG, They conducted H-NMR and FTIR analyses [27].

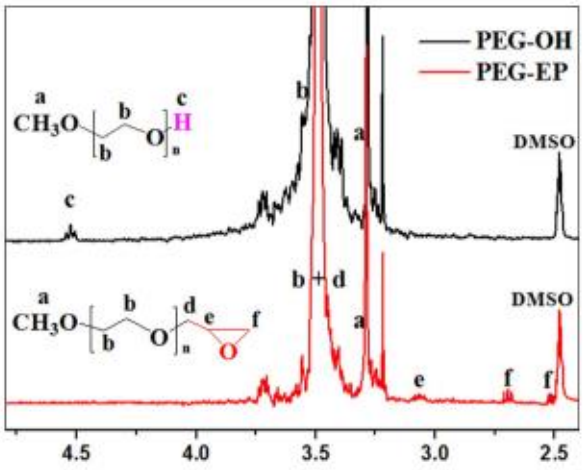

Figure 3.22: H-NMR analysis of PEG-OH and PEG-EP [27].

As seen in Figure 3.22, hydroxyl adsorbance can not be observed in PEG-EP spectrum. According to other peaks in H-NMR analysis and FTIR analysis, the modification was achieved successfully [27].

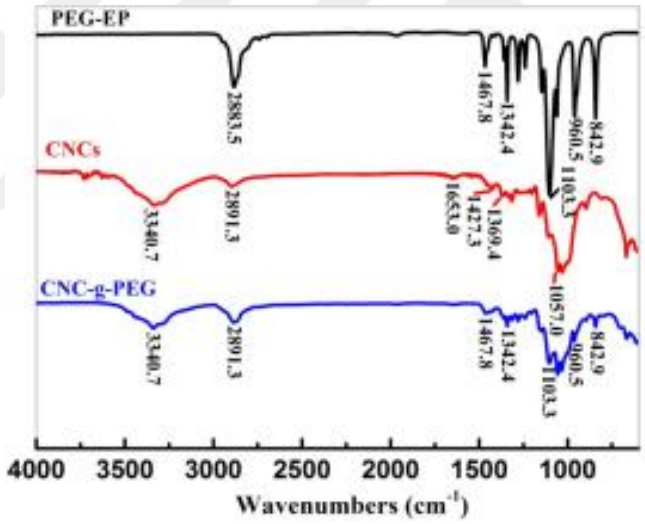

Figure 3.23: FTIR analysis of PEG-EP, CNC and CNC-g-PEG [27].

As seen in Figure 3.23, modified CNC and neat CNC showed almost the same peaks in the FTIR analysis due to similarities in their chemical structures [27].

As well as, they performed thermal analysis to get information about glass transition temperature (Tg), cold crystalization temperature (Tc) and melting temperature (Tm) of PLA and PLA nanocomposites as seen in Figure 3.24 and Table 3.3 [27].

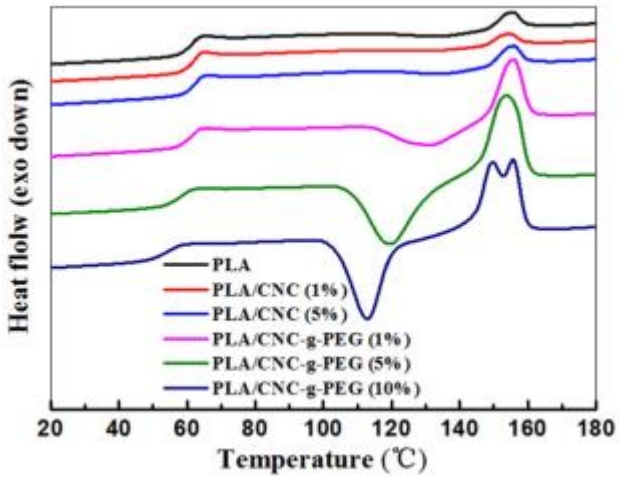

Figure 3.24: DSC analysis of PLA and PLA nanocomposites [27].

Although Tg did not change with the addition of neat CNC in polymer matrices, it decreases by using CNC-g-PEG as a nanofiller in PLA matrices [27].

Table 3.3: Thermal properties of PLA,PLA/CNC and PLA/CNC-g-PEG specimens [27].

Samples	**T_g (°C)**	**T_{cc} (°C)**	**T_m (°C)**	**ΔH_{cc} (J/g)**	**ΔH_m (J/g)**
PLA	61.7	134.5	155.2	2.5	2.8
PLA/CNC (1%)	62.4	134.7	154.8	1.6	1.9
PLA/CNC (5%)	62.5	134.9	155.1	2.4	3.5
PLA/CNC-g-PEG (1%)	61.6	131.5	155.4	12.4	13.2
PLA/CNC-g-PEG (5%)	58.5	120.0	154.2	26.4	26.5
PLA/CNC-g-PEG (10%)	54.8	113.1	149.2, 155.6	26.1	26.9

They obtained the lowest Tg value that is 54.8 °C for PLA/CNC-g-PEG (10%). This is explained by the miscibility of PLA and PEG and low molecular weight PEG behaved like a plasticizer. In the presence of PEG, chain mobility increases for PLA. Also, cold crystalization temperature decreased with the increasing amount of CNC-g-PEG. In their opinion, Tc was decreased because of the increase of dispersion in PLA matrices [27].

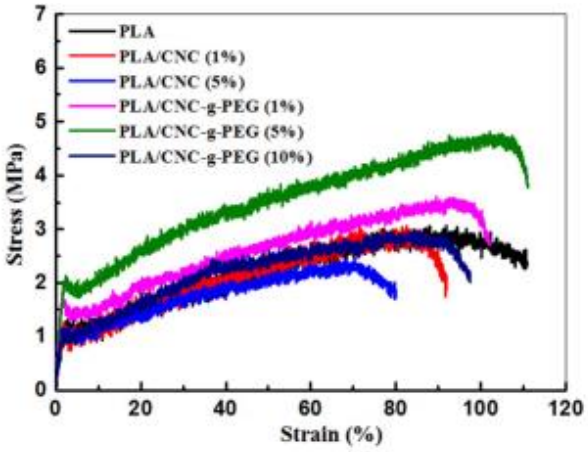

Figure 3.25: Stress strain diagram for PLA, PLA/CNC and PLA/CNC-g-PEG specimens [27].

Also, they conducted tensile tests of PLA and its nanocomposites, and consequently, they analyzed the mechanical properties of these materials. Especially, they investigated elongation at break and ultimate tensile strength. As seen in Figure 3.25, a stress-strain curve was obtained for PLA and its nanocomposites. They did not show any increase in PLA/CNC specimens because of the poor interface between filler and polymer matrices. Also, the ductility of specimens decreased with the addition of neat CNC. PLA is more ductile than PLA/CNC specimens. By adding CNC-g-PEG, specimens had a positive change in mechanical properties. As seen in Figure 3.25 and Table 3.4, the percolation threshold is almost 5% [27].

Table 3.4: Mechanical properties of PLA and PLA nanocomposites [27].

Samples	σ_{max}(MPa)	ε_b(%)
PLA	2.8± 0.4	95± 14
PLA/CNC (1%)	2.8± 0.5	85± 10
PLA/CNC (5%)	2.3± 0.5	71± 11
PLA/CNC-g-PEG (1%)	3.5± 0.2	95± 12
PLA/CNC-g-PEG (5%)	4.7± 0.3	106± 9
PLA/CNC-g-PEG (10%)	2.8± 0.3	91± 10

Improving of the mechanical properties can be related to the presence of a better interface between PLA and CNC-g-PEG. In addition to enhanced properties, they obtained promising properties for using bone tissue engineering in this study [27].

Although using CNC as a nanofiller in hydrophobic polymer matrices is a very important challenge, studies for hydrophilic matrices exist in the literature. PVA/CNC is a good example of these studies [28].

Zheng et al. also studied PEG grafting on CNC surface for use in polyvinyl alcohol (PVA) matrices. In this study, modification of CNC was performed by a different experimental procedure from the previous study. Dopamine which was given in Figure 3.26 was used for PEG modification [28].

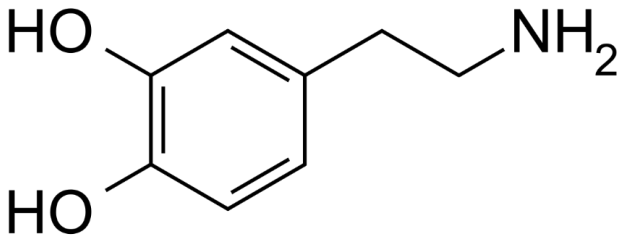

Figure 3.26: Chemical structure of dopamine

Polydopamine (PDA) was obtained in the presence of Tris-HCl and consequently, PDA coated CNC surface was attained to be used for grafting of PEG. To modification of CNC, they used NH_2 terminated PEG with different chain lengths [28].

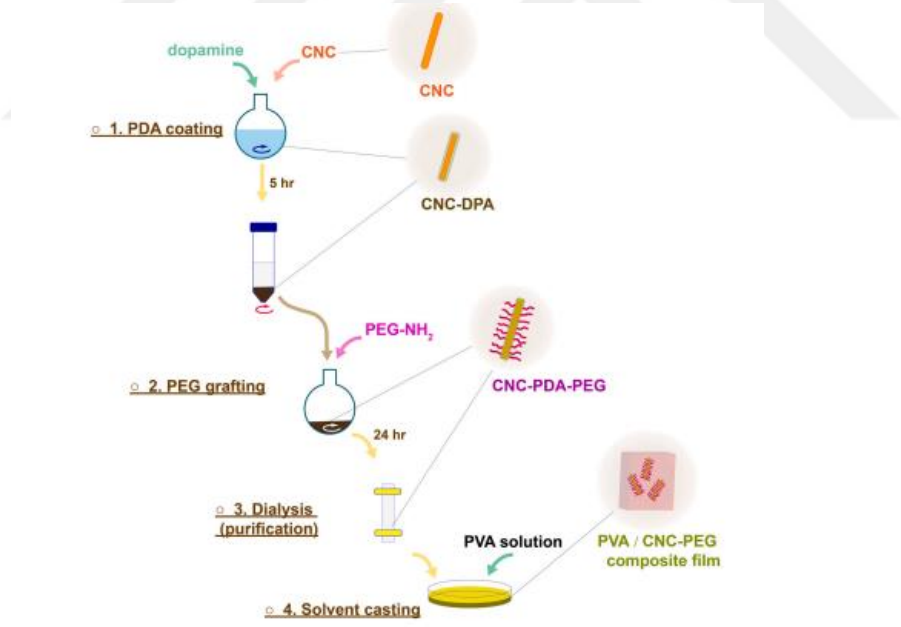

Figure 3.27: Preparation of PVA/CNC-g-PEG [28].

The steps of preparation of PVA/CNC-g-PEG can be seen in Figure 3.27. In this study, PVA/CNC-g-PEG specimens were prepared with solution casting [28].

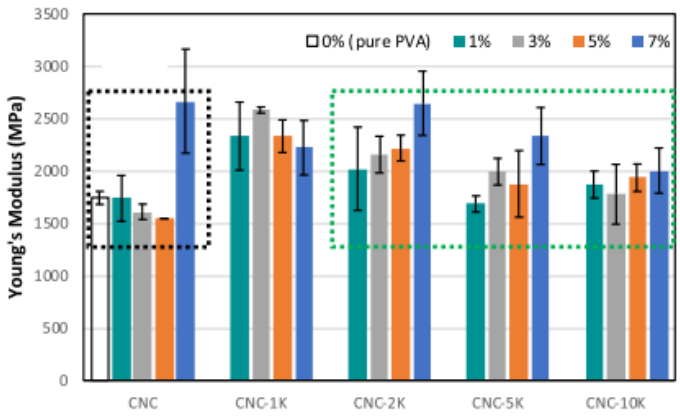

Figure 3.28: Elastic modulus of PVA specimens [28].

They investigated the mechanical properties of PVA specimens that include modifed CNCs by using PEG with different lengths. In the PVA/CNC-g-PEG specimens, Young Modulus generally decreased with increasing PEG chain length as seen in Figure 3.28. This is explained by decreasing matrix and filler interactions as a consequence of more chain entanglement.

In a different study about PEG grafting, NH_2 terminated PEG was used for modification of cellulose microcrystal.

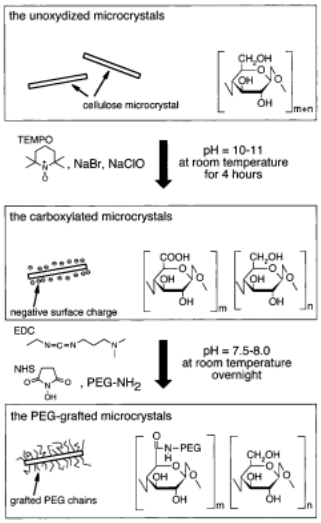

Figure 3.29: Experimental steps for PEG grafting on cellulose microcrystals [29].

As seen in Figure 3.29, modification experiments took place in 2 steps that are TEMPO mediated oxidation and amidation of cellulose structure. They explained why NH_2 terminated structure is used for modification. According to this explanation, amide linkages are more stable than ester linkages [29].

Jeffamine grafted CNC (CNC-g-Jeffamine) is another example of grafting onto method. In the literature, there are some studies on CNC-g-Jeffamine. Jeffamine is an amine-terminated copolymer and its chemical structure take place with ethylene oxide and propylene oxide. Azzam et al. investigated thermoresponsive aggregation properties of modified CNC and used three different Jeffamine that are M1000, M2070 and M2005 [30].

In a different study about CNC-g-M2005, nanocomposite films were prepared with different polymer matrices that are TPS and poly(3- hydroxybutyrate) (P3HB) and investigated mechanical and barrier properties of these films. Before the modification of M2005, TEMPO-mediated oxidation was performed to obtain oxidized CNC. After that, Jeffamine was grafted on CNC surface with an amine-acid coupling reaction. In addition to CNC-g-M2005, sulfated and oxidized CNC was used for producing nanocomposites [31].

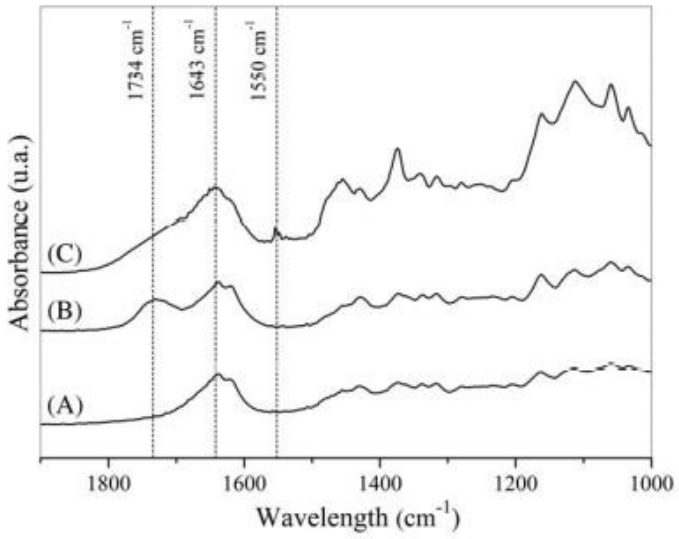

Figure 3.30: FTIR analysis of A) sulfated, B) carboxylated and C) M2005 grafted cellulose nanocrystal [31].

As seen in Figure 3.30, carboxylated CNC showed a peak at 1734 cm-1. With M2005 grafting on CNC, the intensity of this peak had an important reduction. Also, peaks at 1643 cm-1 and 1550 cm-1 are related to amine bonds, they thought modification occurred successfully [31].

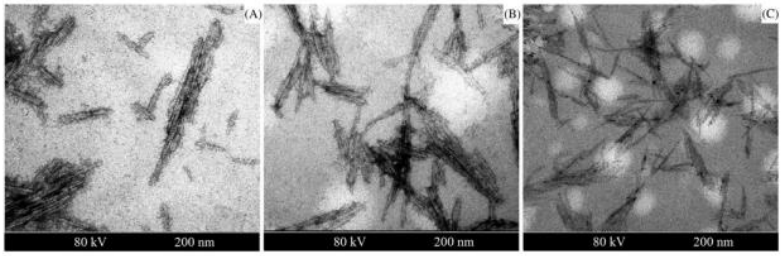

Figure 3.31: TEM analysis of A) sulfated,B) carboxylated and C) M2005 grafted CNC [31].

TEM analysis was performed to understand the morphology of nanocomposite film and consequently, more aggregates are observed in sulfated CNC. As seen in Figure 3.31, a better dispersion was obtained in M2005 grafted CNC. Because M2005 polymer chains enable to increasing of entropic repulsion between CNC [31].

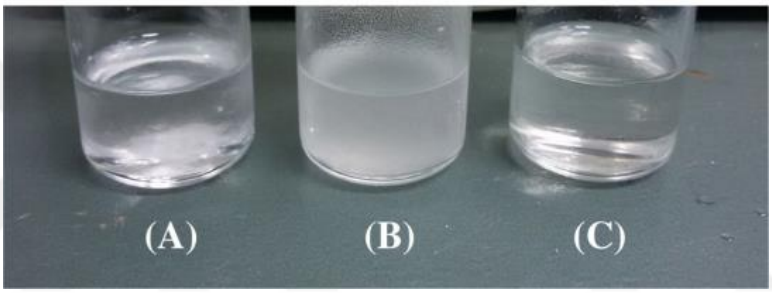

Figure 3.32: Dispersion of CNCs A)sulfated B) carboxylated and C) M2005 grafted in chloroform [31].

Solubility analysis was conducted in chloroform solvent at 60 rpm for 2 minutes as shown in Figure 3.32. Although sulfated CNC did not disperse in the solvent, M2005 grafted CNC could be dispersed. Also, a solution that includes carboxylated CNC was seen as cloudy. It can be a sign of decreased hydrophilicity with modification of CNC [31].

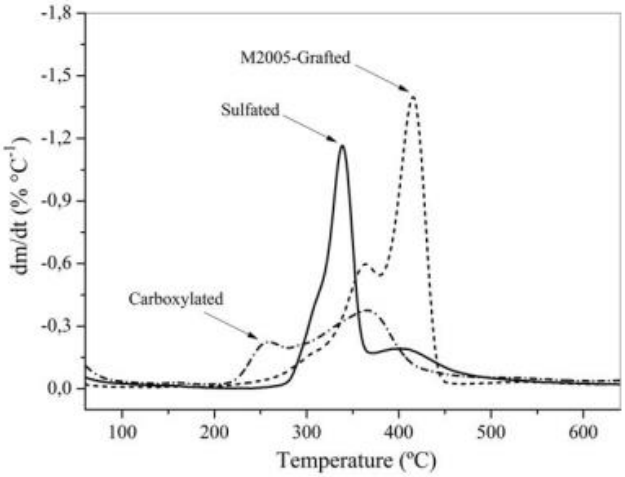

Figure 3.33: Derivative of thermogravimetric analysis for sulfated, carboxylated and M2005 grafted CNC [31].

As seen in Figure 3.33, the onset and maximum degradation temperatures were determined by derivative of TGA. When looking T_{onset} values, CNC-g-M2005 is more stable than sulfated one but, carboxylated CNC is more stable than CNC-g-M2005. Besides CNC-g-M2005 has the highest maximum degradation temperature [31].

Table 3.5: Mechanical properties of TPS, P(3HB) and their nanocomposites [31].

Nanocomposite Film	E (GPa)	TS (MPa)	ε (%)
TPS	1.41±0.62	0.93±0.32	169.51±2.03
TPS/$CNC_{sulphated}$	7.78±0.57	2.71±0.21	128.42±1.88
TPS/$CNC_{carboxylated}$	4.11±1.11	1.51±0.45	97.76±2.22
TPS/CNC_{M2005}	0.84±0.12	0.78±0.36	44.31±1.02
P(3HB)	1.59±0.56	36.05±1.62	8.76±1.01
P(3HB)/$CNC_{sulphated}$	1.89±0.21	42.32±1.76	6.21±1.15
P(3HB)/$CNC_{carboxylated}$	2.02±0.85	48.11±1.53	4.81±1.17
P(3HB)/CNC_{M2005}	3.48±0.74	56.87±1.03	3.32±1.02

As a result of hydrophilic nature of TPS, it gives good interaction with CNC. Also, M2005 chains cause to decreasing of interaction between CNC and TPS. This can be proved by mechanical results as given in Table 3.5. On the other hand, elastic modulus and tensile strength increased with M2005 modification for P3HB polymer [31].

3.7.2 Grafting from

Spinella et al. conducted polymethyl methacrylate (PMMA) grafting on CNC surface in two different ways as given in Figure 3.34. In the first one, Fenton's reagent was used and the reaction took place at 70 ^{o}C for 2 hours. The reaction was performed under nitrogen and water was used as the reaction environment. The second one was conducted by using ceric ammonium nitrate (CAN) as an initiator. This modification reaction took place at 25 ^{o}C for 2 h under nitrogen environment [32].

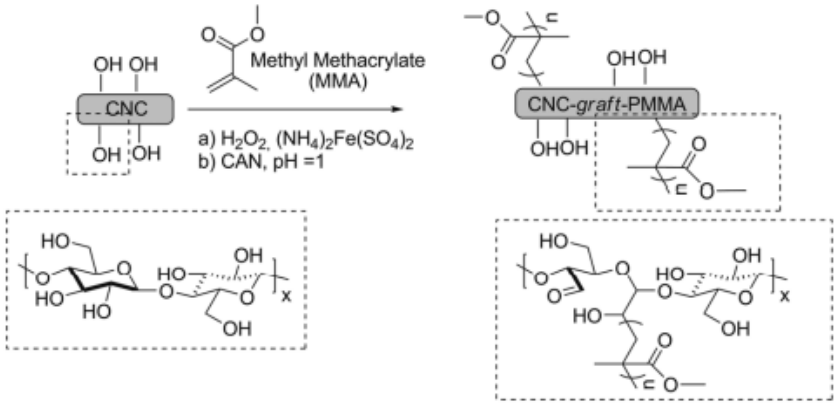

Figure 3.34: PMMA grafting on CNC surface with grafting from method [32].

Following the modification step, PLLA/CNC (5%) nanocomposites were produced with melt extrusion method.

In this study, weight fraction of grafted PMMA was determined by following formula:

$$\frac{m_1 - m_2}{m_1} \times 100 \tag{3.2}$$

m_1 is mass of the modified CNC and m_2 is the initial mass of neat CNC. They conducted FTIR and NMR analysis to understand the chemical structure of modified CNC [32].

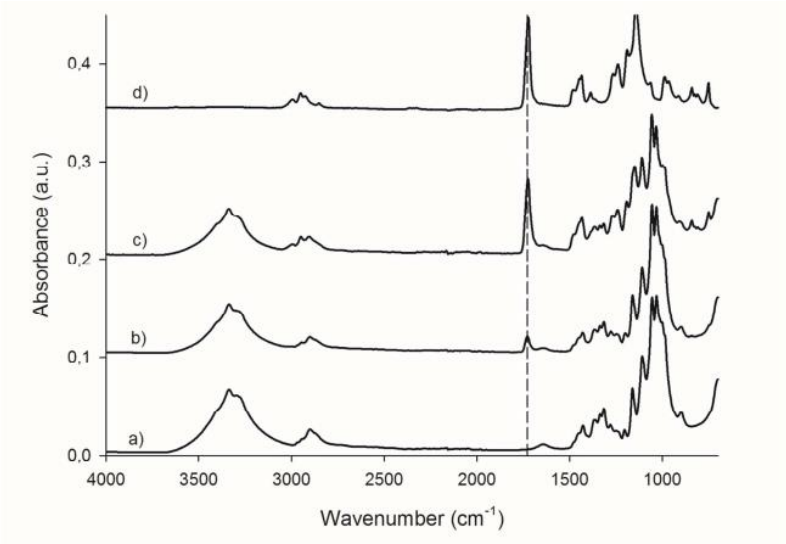

Figure 3.35: FTIR analysis of a) neat CNC b) CNC-g-PMMA$_{15}$, c) CNC-g-PMMA$_{50}$ and d) neat PMMA [32].

New peaks were observed at 1724, 1152, 950 and 750 cm^{-1} with modified CNCs as seen in Figure 3.35. Also, TEM analysis was performed to observe the morphology and consequently, agglomeration decreased with modification of CNC as seen in Figure 3.36 [32].

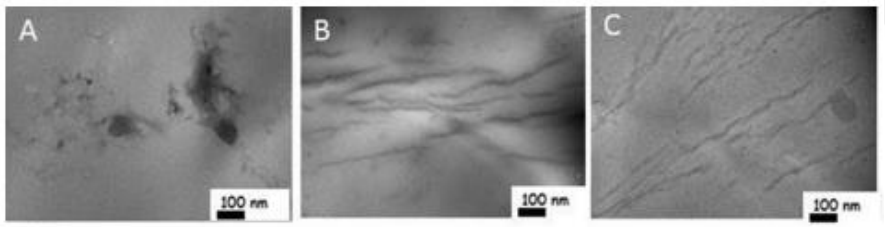

Figure 3.36: TEM images of A) PLLA/CNC, B) PLLA/CNC-g-PMMA$_{15}$ C) PLLA/CNC-g-PMMA$_{50}$ nanocomposites

Nanocomposites that included 5 % of CNC were prepared by injection molding and annealing was applied for 2 hours at 130 ^{o}C. They did not observe significant changes for Tm and Tg in these nanocomposites as given in Table 3.6. Also crystallinity amount (%) slightly decreased with addition of modified CNC. As seen in Table 3.6, the half time of crystallization at 130 ^{o}C decreased by introducing neat CNC. However, the addition of modified CNC led to an increase in half time of crystallization [32].

Table 3.6: Thermal properties of PLLA, PLLA/CNC and PLLA/CNC-g-PMMA specimens [32].

Samples	**T_f (°C)**	**X_c (%)**	**$t_{1/2\text{-}130^oC}$ (min)**	**T_g (°C)**
Neat PLLA	168.1	46.0	18.1	59.1
PLLA/CNC	169.4	49.0	2.7	56.0
PLLA/CNC-g-$PMMA_{15}$	169.4	45.1	7.9	56.7
PLLA/CNC g-$PMMA_{50}$	169.7	42.0	25	58.7

Also, rheological experiments were conducted in the viscoelastic region (strain is about 0.1). According to frequency-sweep test, an increase was observed in storage modulus of PLLA/CNC-g-$PMMA_{50}$ as seen in Figure 3.37 [32].

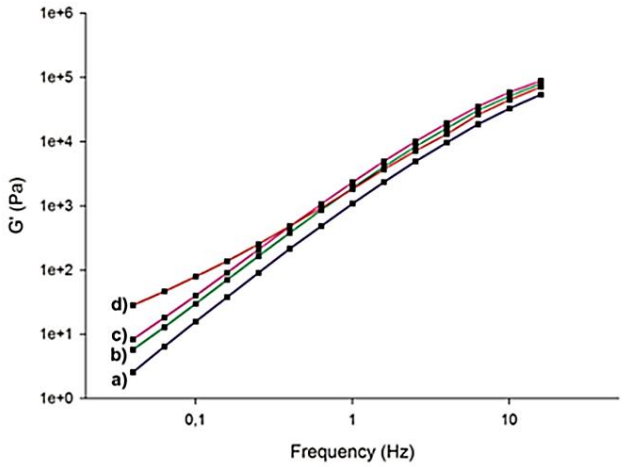

Figure 3.37: Storage modulus (G′) by dynamic rheology at 180 °C, CNC concentration 5%-by-weight on compression-molded specimens for neat PLLA (a), PLLA/CNC (b), PLLA/CNC-g-PMMA15 (c) and PLLA/CNC-g-PMMA50 (d) [32].

However, a significant change was not observed in PLLA/CNC-g-$PMMA_{15}$ as seen in Figure 3.37. In addition, tan δ value decreased with increase of weight fraction of PMMA on CNC surface as seen in Figure 3.38.

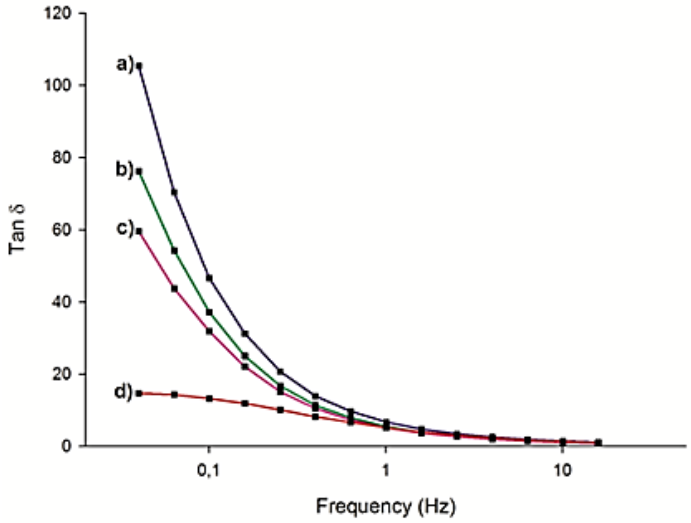

Figure 3.38: tan δ as a function of frequency evaluated by dynamic rheology at 180 °C, CNC concentration 5%-by-weight on compression-molded specimens for neat PLLA (a), PLLA/CNC (b), PLLA/CNC-g-PMMA15 (c) and PLLA/CNC-g-PMMA50 (d) [32].

In addition PLLA nanocomposite, PMMA grafting on CNC was studied for using in PMMA matrices. CAN was used as initiator to synthesize PMMA as given in Figure 3.39.

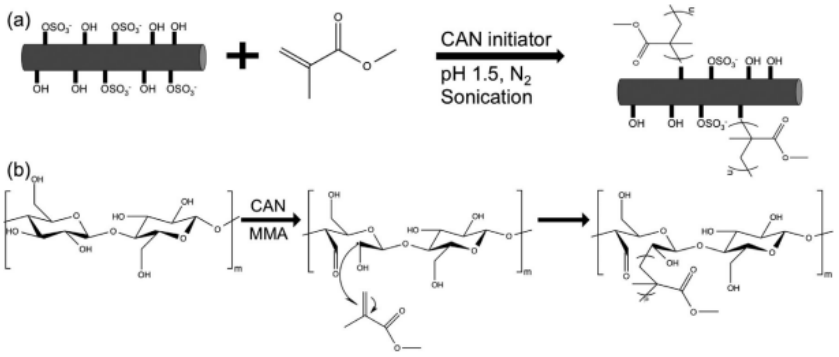

Figure 3.39: a) First step b) Second step of CNC modification [33].

After the grafting step, FTIR and NMR analyses were conducted to analyze the chemical structure of modified and unmodified CNCs. They observed significant changes between neat CNC and CNC-g-PMMA. The peak at 1730 cm^{-1} was observed and it represents C=O bonds as given in Figure 3.40.

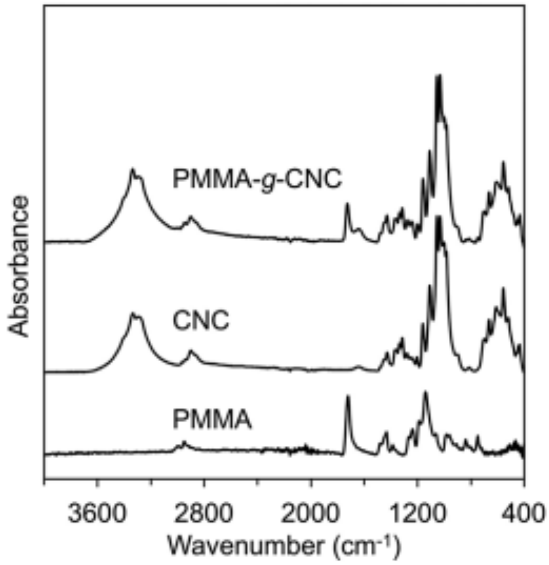

Figure 3.40: FTIR analysis of PMMA,CNC and CNC-g-PMMA [33].

Nanocomposites were produced with two methods that are melt mixing and ball milling. Specimens can be seen in Figure 3.41. Compare to ball milling specimens, melt mixing specimens have more color changing, especially the highest amount of CNC-g-PMMA. This was explained by the formation of sulphuric acid and causing of the hydrolization of CNC [33].

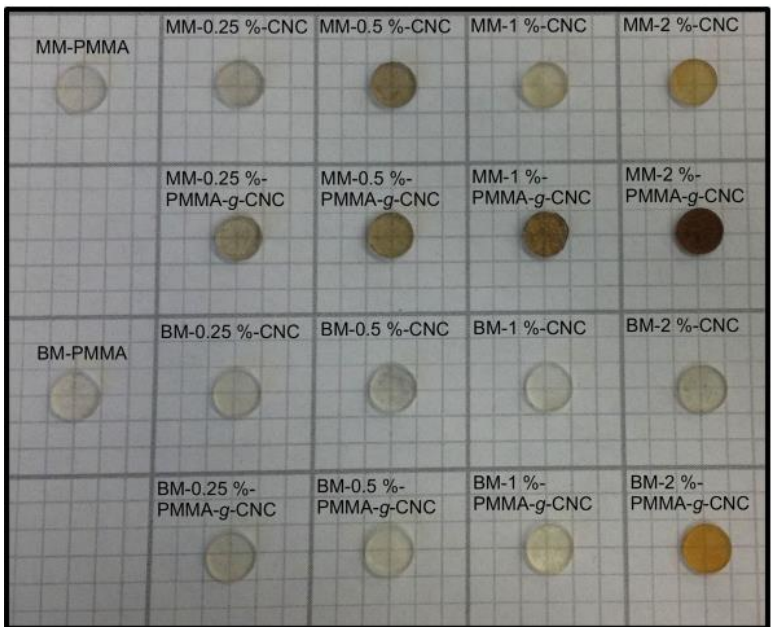

Figure 3.41: Specimens that were produced with melt mixing and ball milling [33].

In this study, mechanical and rheological properties were analyzed by using a tensile tester and rheometer. They did not observe important changes in rheological and mechanical properties [33].

Besides PMMA grafting, studies about Poly(L-lactide)(PLLA) and Polycaprolactone (PCL) are commonly used for grafting of CNC. In a study, CNC was modified with PLLA and PCL as seen in Figure 3.42. This study was really important because it gives information about potential applications of biodegradable polymers such as packaging and biomedicine [34].

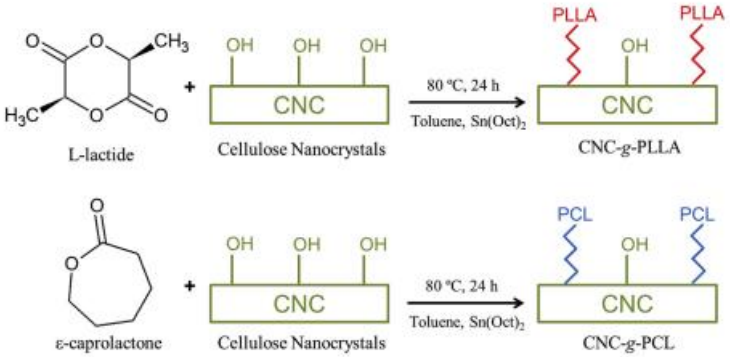

Figure 3.42: PLLA and PCL modification of CNCs [34].

PLLA/PCL blends were prepared with 70:30 ratio and 1 wt. % of modified and unmodified CNC were added in these blends as a filler [34].

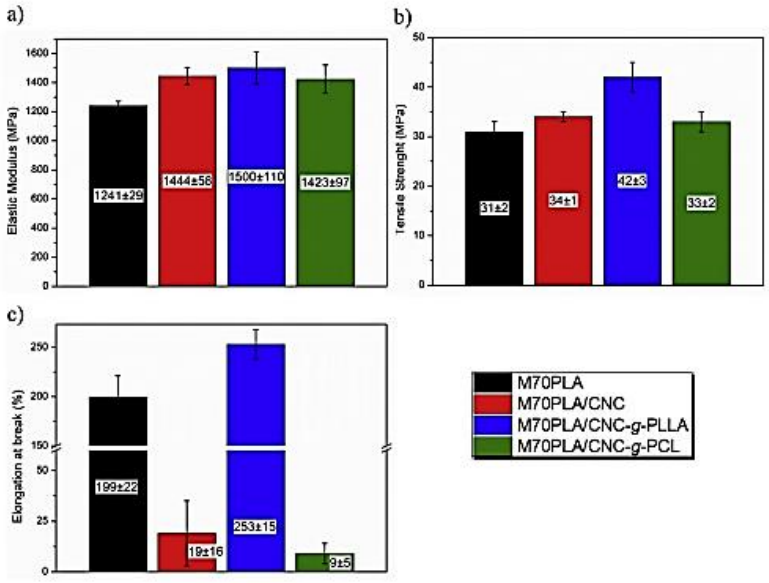

Figure 3.43: Mechanical results of PLA/PCL blends and CNC based nanocomposites [34].

With the addition of CNC, elastic modulus and tensile strength increased but elongation at break decreased. On the other hand, elongation at break increased dramatically by using CNC-g-PLLA however, CNC-g-PCL is the worst filler to obtain good ductility as seen in Figure 3.43 [34].

Le Gears et al. studied PGMA modification on CNC surface by using atom transfer radical polymerization and produced PLA/CNC specimens by solvent casting method. In this study, they focused on SEM analysis to understand changes in the agglomeration of CNCs in the PLA matrix and they mentioned about development with the addition of modified CNCs.

4. EXPERIMENTAL PROCEDURE

4.1 Materials

Spray Dried Cellulose nanocrystal was provided by Celluforce from Canada. Glycidyl methacrylate (GMA) was purchased from Sigma Aldrich and purified through a neutral alumina column to remove stabilizers before use. Potassium persulfate (KPS) was purchased from Sigma Aldrich. Methanol with 99% provided by Sigma Aldrich. PBAT which is ecoflex F Blend C1200 was provided by BASF. O

4.2 Synthesis of Neat PGMAs

PGMA was synthesized under the conditions which are given in Table 4.1. Before the addition of GMA, the temperature was set to 70 ^{o}C and KPS was added to the reaction environment. Then different amounts of GMA were introduced into the reaction environment for each PGMA synthesis. And these polymers were named according to the concentration of GMA. For instance, when 5 ml of GMA was added to 50 ml of distilled water, it is called CNC-g-PGMA5.

Table 4.1: Neat PGMA specimen synthesis.

Amount of the Initiator	Amount of GMA per 50 ml of water	Reaction Conditions	PGMA Specimens
0.1 g KPS	0.5 ml	3 hours 70 ^{o} C	PGMA0.5
	1 ml		PGMA1
	5 ml		PGMA5
	10 ml		PGMA10

4.3 Synthesis of CNC-g-PGMAs

In this step, CNC was modified with PGMA as seen in Figure 4.1 and modified CNCs. Reaction conditions are shown in Table 4.2. 1 g of CNC was added to 50 ml of distilled water and the mixture was stirred until a good dispersion in water was obtained. After that, the reflux flask system was prepared and the temperature was set to 70 ^{o}C. The reaction setup is given in Figure 4.2. Before the addition of 0.1 gram of KPS, the reaction environment was purged by using nitrogen gas. Then GMA was added to the reaction environment slowly with different amounts that are 0.5, 1, 5 ml. The reaction took place for 3 hours at 70 ^{o}C and methanol was added to terminate the modification reaction. After the reaction termination, the centrifugation step was performed by using water and acetone.

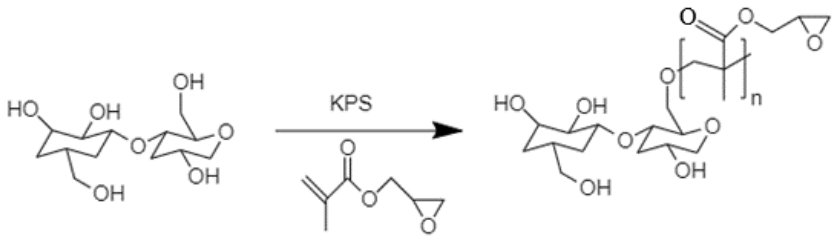

Figure 4.1: PGMA modification on CNC surface by using KPS as initiator and GMA as a monomer.

Then, the product was stirred for 24 hours in THF solvent to get rid of homopolymer which can not give a chemical reaction with CNC. After this step, specimens were dried in a vacuum oven and the remained weight was measured. Remained product was introduced in THF again and it was stirred for 24 hours. When nearly the same weight was measured, the specimen was dried and prepared for the production of the nanocomposite step.

Table 4.2: CNC-g-PGMA specimens and reaction conditions.

Amount of CNC per 50 ml of water	Amount of the Initiator	Amount of GMA per 50 ml of water	Reaction Conditions	CNC-g-PGMA Specimens
1 g of CNC	0.1 g KPS	0.5 ml	3 hours 70 ^{o}C	CNC-g-PGMA0.5
		1 ml		CNC-g-PGMA1
		5 ml		CNC-g-PGMA5

Figure 4.2: Experimental setup for PGMA modification on CNC surface.

4.4 Production of PBAT Nanocomposites

Neat PBAT, PBAT/CNC, and PBAT/modified CNC specimens were produced by using a melt mixer as seen in Table 4.3. In this step, the temperature was set to 160 o C. Also screw speed and process time were determined at 100 rpm and 5 minutes. PBAT/CNC specimens were prepared with 3 wt.% of spray dried CNC. Firstly, PBAT granules were added to the melt mixer then, CNCs were introduced. The same stages were applied to produce the PBAT/CNC-g-PGMA specimens. Neat PGMAs which are PGMA0.5, PGMA1, and PGMA5 were used with the same amount to compare the effects of CNC-g-PGMA and neat PGMA.

Table 4.3: Production of PBAT/CNC-g-PGMA and PBAT/PGMA.

Specimens	Process Conditions	Preparation of Rheology Specimens
PBAT/CNC-g-PGMA0.5	100 rpm 5 minutes 160 °C	1.5 psi 5 minutes 160 °C
PBAT/CNC-g-PGMA1		
PBAT/CNC-g-PGMA5		
PBAT/PGMA0.5		
PBAT/PGMA1		
PBAT/ PGMA5		
PBAT/PGMA10		

4.5 Characterization

In this step, firstly FTIR analysis was performed to understand the chemical structure. To determine the molecular weight of PGMA on the CNC surface, solvents were prepared for GPC. However, the specimens did not dissolve in THF. Also, TGA and DSC analyses were conducted to determine thermal properties and rheological properties were determined by rheological tests.

4.5.1 FTIR analysis

FTIR spectra of the neat CNC and modified CNCs prepared and recorded at room temperature in the mid-IR range (400 – 4000 cm^{-1}) by using a Bruker FTIR spectrometer equipped with a Bruker Platinum ATR accessory. All of the measurements were performed after vacuum drying.

4.5.2 Thermogravimetric analysis (TGA)

TGA was conducted under nitrogen environment with heating rate of 10 °C/min from room temperature to 700 °C using TA instruments with TGA Q50 apparatus. Neat CNC and modified CNCs were analyzed with TGA.

4.5.3 Differential scanning calorimetry (DSC)

PBAT/CNC specimens were analyzed by using DSC to determine thermal behavior. It was performed from room temperature to 200 ^{o}C at a heating rate of 10^{o}C/min with 3 steps which are 1st heating, cooling and 2nd heating.

4.5.4 Rhelogical analysis

Rheological analysis were performed with MCR-301 rotational rheometer (Anton Paar, Austria) as shown in Figure 4.3. Rheological results were obtained at 160 ^{o}C under the nitrogen environment. Frequency-sweep tests were conducted from 0.1 to 628 rad/s to determine rheological properties which are storage modulus and complex viscosity. It could give information about dispersion of CNC in PBAT matrix.

Figure 4.3: Anton Paar MCR 301 rheometer.

5. RESULT AND DISCUSSION

5.1 Effects of GMA Concentration without CNC

FTIR analysis makes it easy to identify the chemical structure and it was performed to analyze neat PGMA specimens as seen in Figure 5.1. Similar peaks were observed in all PGMA specimens. Peaks at 1730 cm^{-1} is related to carbonyl groups and this group is a part of PGMA chains.

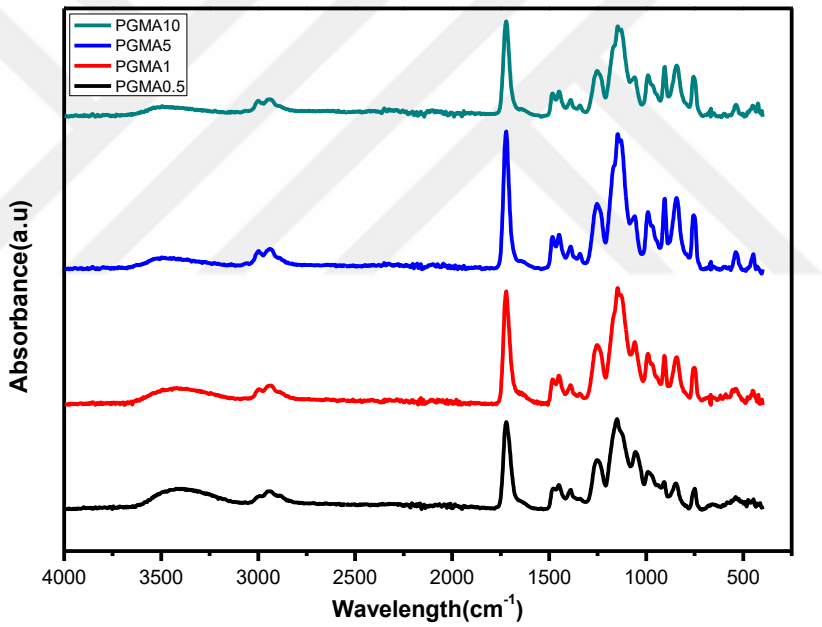

Figure 5.1: FTIR analysis of PGMA0.5, PGMA1, PGMA5 and PGMA10.

To understand the effects of PGMA on the PBAT matrix, PBAT/PGMA specimens were produced with 3 wt.% of PGMAs. Rheological analysis was conducted and the results are given in Figure 5.2 and Figure 5.3. With the addition of PGMA, remarkable changes were noted. When the GMA concentration decreased, rheological properties increased dramatically, except for the PGMA0.5. PBAT/PGMA0.5 did not have any important change in rheological properties. This situation can be explained by insufficient monomer amount for obtaining long chains whereas, good results usually

were not obtained with increasing the concentration. As the higher concentration of GMA causes more interaction and entanglement between PGMA chains also gellation can occur under synthesis conditions.

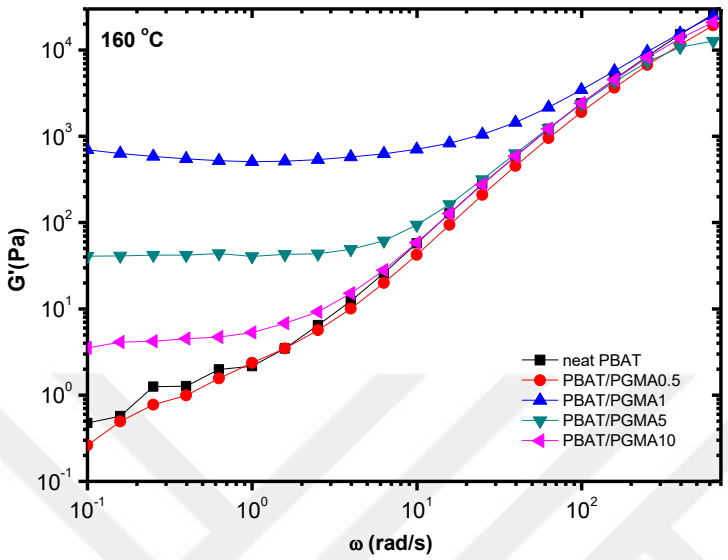

Figure 5.2: Storage modulus as a function of frequency for neat PBAT and PBAT/PGMA specimens.

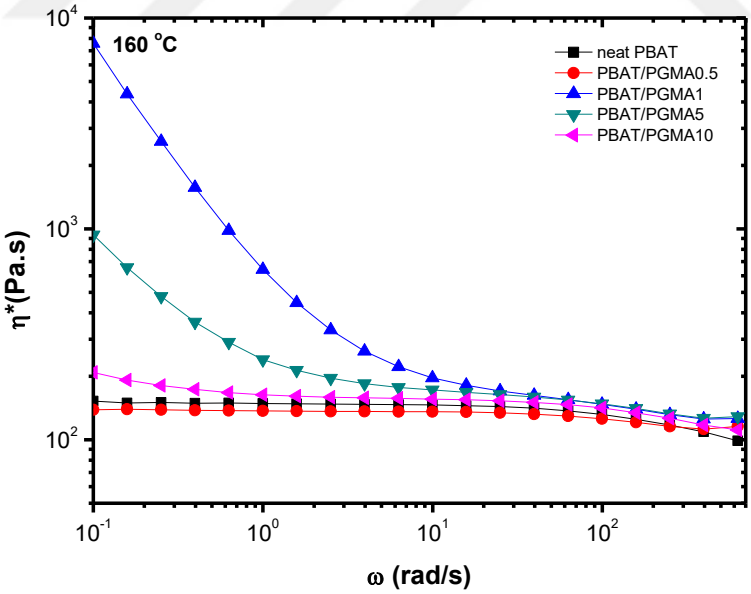

Figure 5.3: Complex viscosity as a function of frequency for neat PBAT and PBAT/PGMA specimens.

5.2 Effects of GMA Concentration with CNC

As seen in Figure 5.4, neat CNC shows a large peak from 3000 cm^{-1} to 3700 cm^{-1} and this peak is related to -OH bonds of hydroxyl groups. Also, -C-O bonds of cellulose repeating unit gave some peaks at approximately 1100 cm^{-1} and 1020 cm^{-1}. With the modification of CNC, the intensity of OH group peaks decreased. Also peak at 1730 cm^{-1} which is related to -C=O vibration band was observed. It means that cellulose nanocrystal was modified successfully by using GMA.

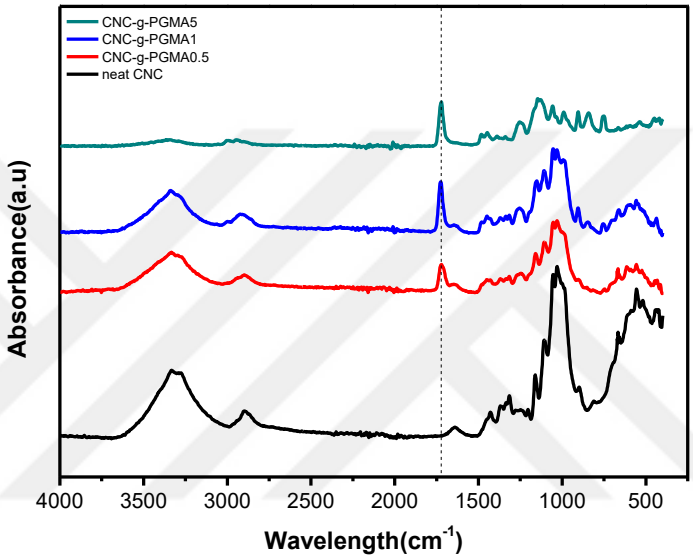

Figure 5.4: FTIR analysis of neat CNC, CNC-g-PGMA 0.5, CNC-g-PGMA1 and CNC-g-PGMA5.

TGA was performed to analyze neat CNC,neat PGMAs and CNC-g-PGMA specimens as given in Figure 5.5. For neat CNC, nearly 7 % of weight loss has been observed until 100 ^{o}C. This could be explained by water content due to hydroxyl groups on the CNC surface. In PGMA modified CNCs, this weight loss was not notable up to 100 ^{o}C. Significant weight loss was started at 280 ^{o} C and remained weight was just 40% at 320 ^{o}C for neat CNC whereas, degradation was started earlier for CNC-g-PGMA0.5 and CNC-g-PGMA1 samples. Small PGMA chains may have caused this. CNC-g-PGMA5 includes two main degradation temperature ranges which are between 200 ^{o}C and 300 ^{o}C and above 300 ^{o}C. At 300 ^{o}C, the remained weight was nearly 80% and it had approximately the same value for 320 ^{o}C. When the PGMA samples were investigated, the weight loss started at the lower temperatures for PGMA0.5 and PGMA1. However, the same weight loss amount which was 15 % was obtained at 300

ºC for all neat PGMA samples. After the 300 ºC, PGMA5 showed higher weight loss rate than other PGMA samples. Neat PGMA samples includes noticable thermal degradation temperature around 400 º C. CNC-g-PGMA samples showed both neat PGMA and CNC properties in TGA whereas, degradation was started earlier for CNC-g-PGMA0.5 and CNC-g-PGMA1 samples because of degredation of small chains. Also, CNC may be damaged due to reaction conditions and insufficient GMA concentration.

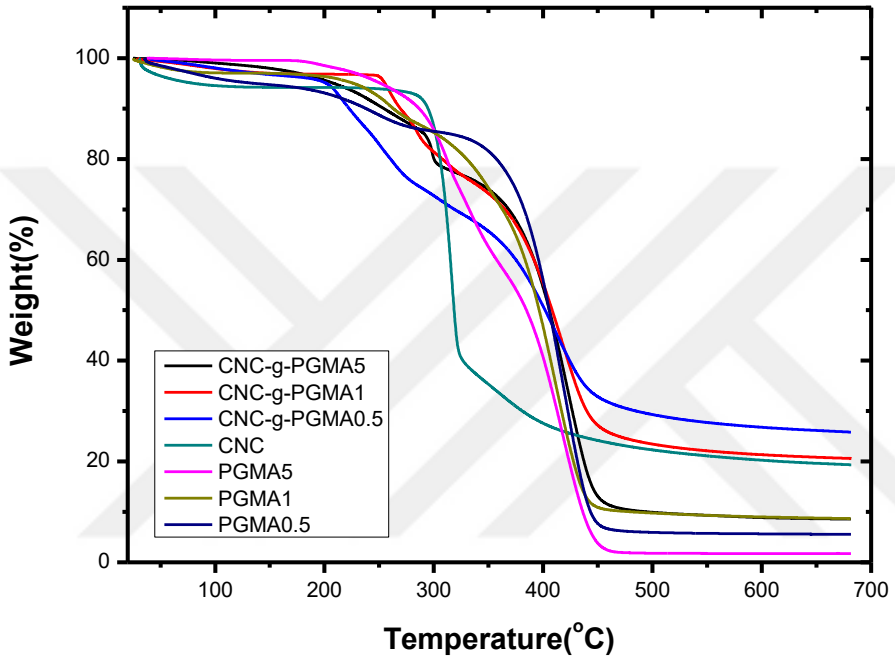

Figure 5.5: Thermogravimetric analysis of neat CNC and modified CNCs.

Rheological results were obtained at the melting phase and these properties can give details about the dispersion of nanofillers in the polymer matrix. Storage modulus and complex viscosity values were determined with the rheological analysis. At high frequencies, knowledge about polymer matrix can be obtained. On the other hand, getting information about molecular interaction between CNCs and polymer matrix is possible since polymers or composites are given enough time to understand molecular interactions as well as it gives details about the dispersion of CNCs. As seen in Figure 5.6 and Figure 5.7, PBAT and PBAT/CNC specimens have the same rheology results at different frequencies. It can be interpreted as the distribution of CNC was not good enough and a good network was not obtained in PBAT. Also, a significant change was not taking place with the addition of CNC-g-PGMA0.5 and CNC-g-PGMA1. PGMA

chains on CNC surface may not reach enough length to bridge between CNCs and PBAT matrix. Despite the undesirable results with CNC-g-PGMA0.5 and CNC-g-PGMA1, CNC-g-PGMA5 has a positive effect on the PBAT matrix. Storage modulus and complex viscosity increased dramatically with the addition of CNC-g-PGMA5 and consequently, strong chemical interaction took place between CNC and PBAT because epoxy rings on PGMA chains contribute to chemical interactions. At process temperature, these rings could open and give chemical reaction with PBAT chains.

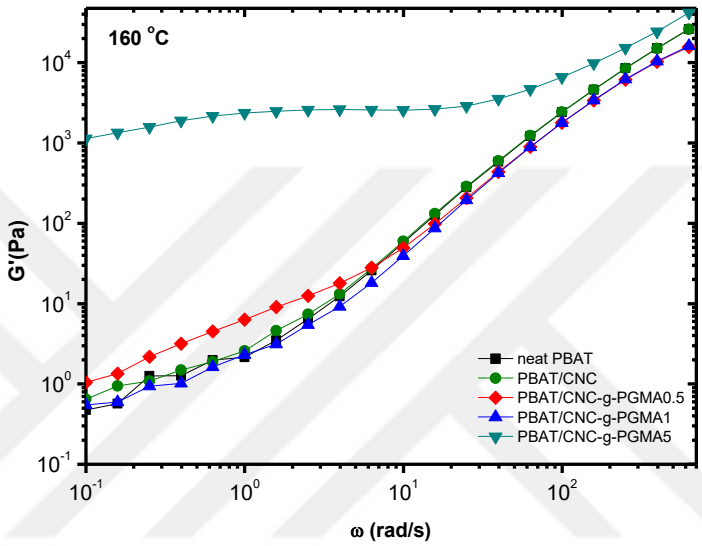

Figure 5.6: Storage modulus as a function of frequency for neat PBAT, PBAT/CNC and PBAT/CNC-g-PGMA specimens.

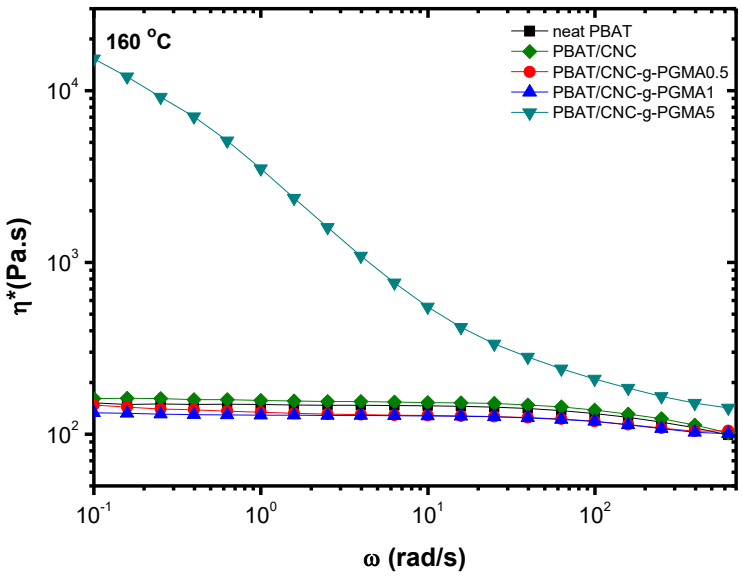

Figure 5.7: Complex viscosity as a function of frequency for neat PBAT, PBAT/CNC and PBAT/CNC-g-PGMA specimens.

The highest rheological results were obtained for CNC-g-PGMA5. In order to compare the effects of CNC-g-PGMA5 and PGMA5, rheological results were determined at different frequencies, and consequently, higher results were obtained for PBAT/CNC-g-PGMA5 as seen in Figure 5.6 and Figure 5.7.

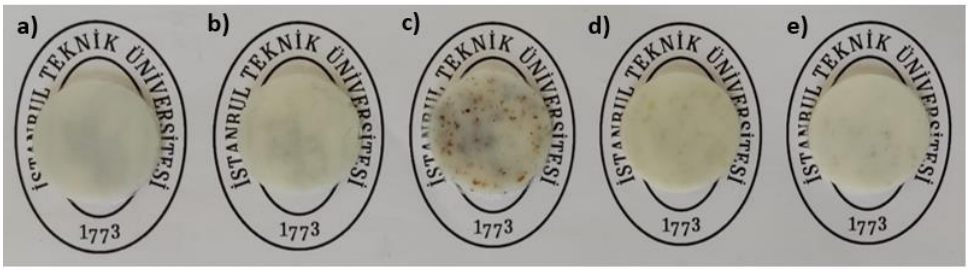

Figure 5.8: Rheology disc of a) PBAT b)PBAT/CNC c) PBAT/CNC-g-PGMA0.5 d) PBAT/CNC-g-PGMA1 and e) PBAT/CNC-g-PGMA5.

Modified CNCs can be affected by process conditions. CNCs can be degraded easily with increasing process temperature. Also in the modification step, CNC gets damaged by reaction conditions. As seen in Figure 5.8, Although PBAT/CNC specimens did not have any color change, dark dots were observed on PBAT/CNC-g-PGMA0.5. On the one hand, the color change was notable on PBAT/CNC-g-PGMA1. On the other hand, any significant color change was not observed with the addition of CNC-g-PGMA5. At high temperatures, molecules on CNC surface without enough chain length can be degraded however, longer chains can not be degraded easily.

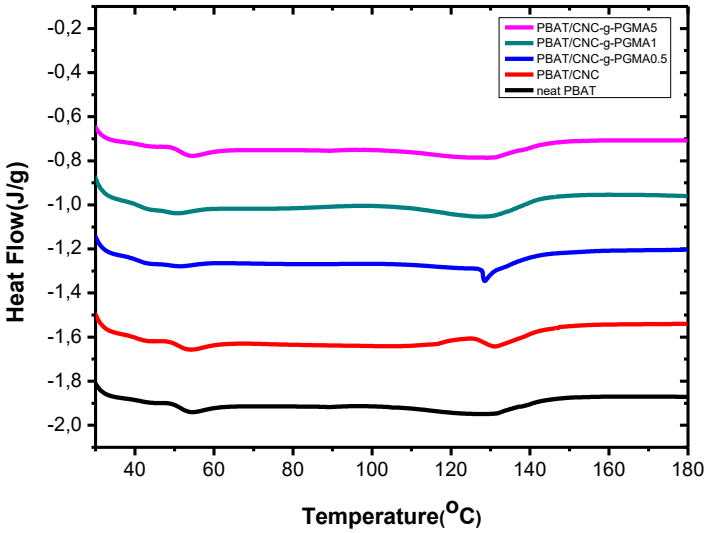

Figure 5.9: DSC first heating thermograms of PBAT, PBAT/CNC, PBAT/CNC-g-PGMA specimens.

The first heating results are shown in Figure 5.9. Differences in the preparation of specimens cause to obtain significant results. To get the best results, the second heating is crucial. Before the second heating, the cooling step was performed as shown in Figure 5.10. The crystallization temperature(Tc) of PBAT increased with adding of neat CNC, CNC-g-PGMA0.5, and CNC-g-PGMA1. However, PBAT/CNC-g-PGMA5 shows the lowest Tc value. With the addition of neat CNC, crystallization could be faster. Also, CNC-g-PGMA0.5 and CNC-g-PGMA1 have a positive effect on crystallization kinetics. However, CNC-g-PGMA5 has a negative effect on crystallization kinetics. It can be explained by decreasing surface area and consequently, CNC could not behave like a nucleating agent.

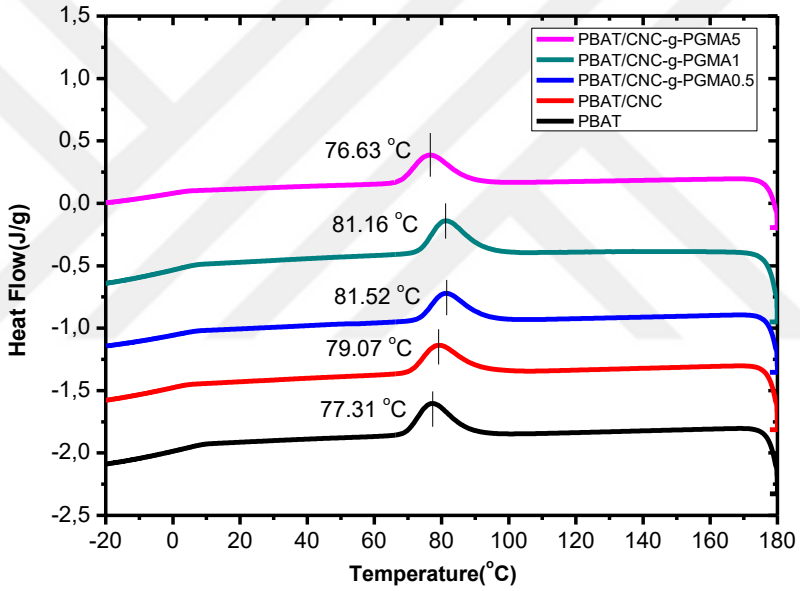

Figure 5.10: DSC cooling thermograms of PBAT, PBAT/CNC, PBAT/CNC-g-PGMA specimens.

In second heating DSC analysis, melting temperatures were determined and slight changes were observed as seen in Figure 5.11. Thanks to these results, crystalinity amount (%) (Xc) was calculated by the following formulas [35]:

$$X_c^{heating} = \frac{(\Delta Hm) \times 100}{w_{PBAT}\, \Delta H_m^0} \tag{5.1}$$

$$X_c^{cooling} = \frac{(\Delta Hc) \times 100}{w_{PBAT}\, \Delta H_m^0} \tag{5.2}$$

(ΔHm) is the melting entalpy and the crystallization enthalpy is called as (ΔHc). W_{PBAT} is the weight fraction of the PBAT and ΔH^0_m is the heat of fusion of 100% crystalline PBAT which is given as 114 J/g [35].

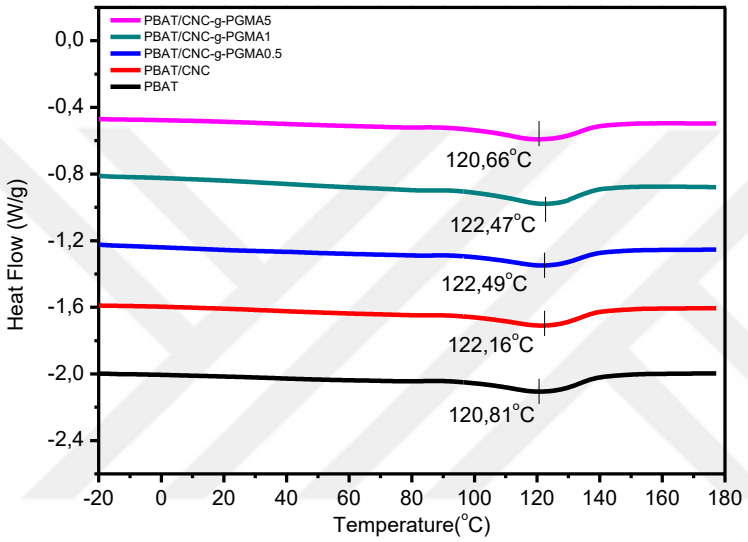

Figure 5.11: DSC second heating thermograms of PBAT, PBAT/CNC, PBAT/CNC-g-PGMA specimens.

Table 5.1: Thermal properties of PBAT, PBAT/CNC and PBAT/CNC-g-PGMA specimens.

Sample	Crystallization and Melting Temperatures		Degree of Crystallinity (%)	
	T_c	T_m	X_c	X_m
Neat PBAT	77.31	120.81	17.28	14.72
PBAT/CNC	79.07	122.16	17.71	13.37
PBAT/CNC-g-PGMA0.5	81.52	122.49	16.23	14.10
PBAT/CNC-g-PGMA1	81.16	122.47	20.38	14.19
PBAT/CNC-g-PGMA5	76.63	120.66	16.64	13.95

In the heating, X_c amount increased with addition of CNC-g-PGMA1 in PBAT matrix as seen in Table 5.1.

5.3 Comparison of PBAT/CNC-g-PGMAs and PBAT/PGMAs

The best results were obtained in PBAT/CNC-g-PGMA5 for PBAT with CNC specimens. Neat CNC did not have any positive effect on rheological properties also CNC-g-PGMA0.5 and CNC-g-PGMA1 show similar rheological properties. However, with the addition of CNC-g-PGMA5, rheological properties had a dramatic increase, especially at low frequencies. To understand the effects of CNC, CNC-g-PGMA5 and PGMA5 can be compared to each other as seen in Figure 5.12. PBAT/CNC-g-PGMA5 has higher complex viscosity and storage modulus values than PBAT/PGMA5. It shows the positive effects of CNC on PBAT specimens. CNC provides a surface for polymerization and polymerization could start from different points at the same time these polymer chains tethered on the CNC surface can provide better interaction between CNC and PBAT matrix. Also, rheological properties increased with the addition of PGMA5 because of reactive epoxy rings. However, the increase is not higher than the addition of CNC-g-PGMA. It can be explained by two main reasons. The first one is better dispersion of CNC enables to obtain better rheological properties. The second one is obtaining the optimum chain length because the CNC surface creates different points for polymerization

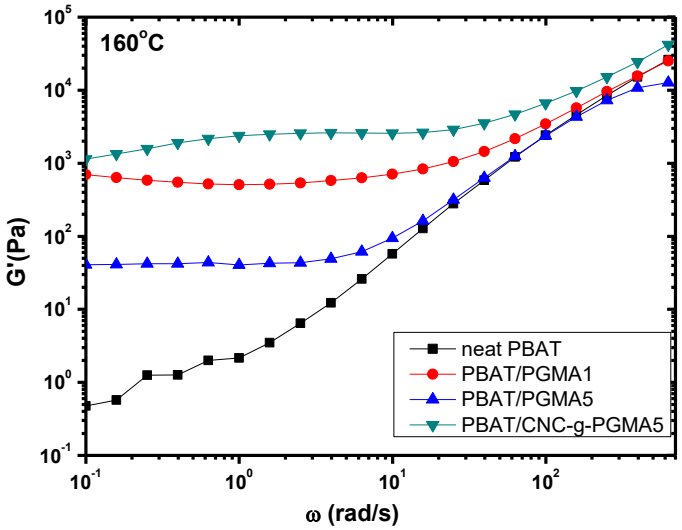

Figure 5.12: Storage modulus at different frequencies for PBAT, PBAT/PGMA1, PBAT/PGMA5 and PBAT/CNC-g-PGMA5 specimens.

PGMA1 shows the best result in neat PGMAs and addition of PGMA1 contributes better development for PBAT matrix and rheological results are close with PBAT/CNC-g-PGMA5.

However, PBAT/CNC-g-PGMA5 shows higher development in rheological results especially for complex viscosity as shown in Figure 5.13. Development of CNC dispersion could be related to this consequence.

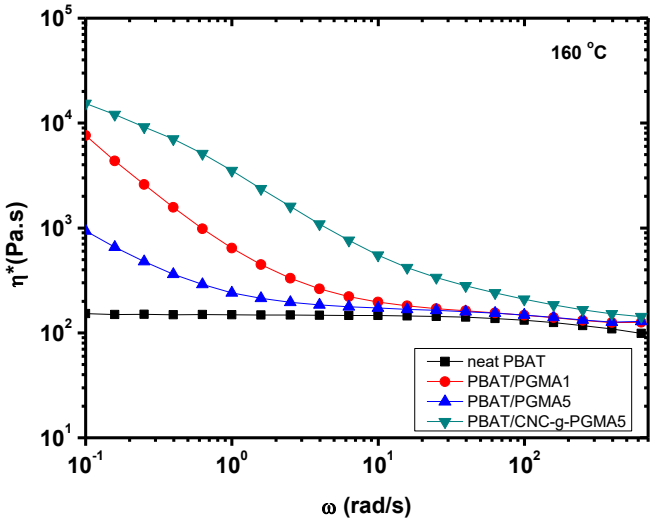

Figure 5.13: Complex viscosity at different frequencies for PBAT, PBAT/PGMA1, PBAT/PGMA5 and PBAT/CNC-g-PGMA5 specimens.

6. CONCLUSIONS

The present work aimed to develop dispersion of CNC in hydrophobic polymer matrices with the melt mixing method. Despite its superior properties such as high mechanical strength, lightweight, and high surface area, agglomeration of CNC is a crucial problem for producing nanocomposites. To solve this problem, CNC was modified by grafting from method and GMA was chosen to polymerize on the CNC surface. Before this step, neat PGMA was synthesized with different GMA concentrations in distilled water and PBAT/PGMA specimens with 3 wt.% PGMA were produced. Thanks to the rheological analysis, PBAT and PGMA interactions were understood. Epoxy rings were opened during the process and gave reaction with PBAT. After this step, CNCs were modified with different GMA concentrations. In FTIR analysis the peak which is related to C=O at 1725 cm-1 was obtained. It means that CNC has PGMA structure on its surface since PGMA includes these groups. Also, TGA was performed for CNC-g-PGMA samples. In CNC-g-PGMA0.5 and CNC-g-PGMA1, degradation temperature decreased. This can be explained by insufficient GMA concentration. 0.1 g of KPS created initiation points for polymerization however GMA concentration was not enough.

PBAT/CNC-g-PGMA specimens were prepared with melt mixing method. In this method, unlike solution casting, the process took place without any harmful solvent such as THF or DMF. It gives information about large-scale production whereas, solution casting is not applicable for mass production.

The best rheological results were obtained in PBAT/CNC-g-PGMA5 specimens whereas, any development was not observed with the addition of CNC-g-PGMA0.5 and CNC-g-PGMA1. Also, black dots were observed in PBAT/CNC-g-PGMA0.5 specimens. Polymerization on the CNC surface took place in every sample but the concentration of GMA was insufficient for CNC-g-PGMA0.5 and CNC-g-PGMA1 and small chains on CNC could be degraded under the process conditions which also explains the undeveloped rheological results. Also, crystallization temperature

decreased with the addition of CNC-g-PGMA5. The longer PGMA chains prevent CNC surface to behave as nucleating agents.

To conclude, rheological results increased in the presence of PGMA without CNC because of the chemical reaction between PGMA and PBAT during the melt mixing process. Also, with the addition of CNC-g-PGMA5, improvement was obtained in rheological results for PBAT nanocomposite compared to neat PBAT and PBAT/CNC specimens. It can be explained by better dispersion of CNC and stronger interface due to the chemical reaction between PGMA and PBAT.

CNC can be a good alternative to use as nanofiller for polymer matrix. Especially, to produce eco-friendly polymer nanocomposites, PGMA modification of CNC is a crucial step for producing CNC nanocomposites without any harmful solvent. PBAT/CNC-g-PGMA nanocomposites have a good future in commodity and biomedical applications as proven by the remarkable results.

REFERENCES

[1] **Tang, J., Sisler, J., Grishkewich, N., & Tam, K. C.** (2017). Functionalization of cellulose nanocrystals for advanced applications. Journal of colloid and interface science, 494, 397-409.

[2] **George, J., & Sabapathi, S. N.** (2015). Cellulose nanocrystals: synthesis, functional properties, and applications. *Nanotechnology, science and applications*, *8*, 45.

[3] **Tavakolian, M., Jafari, S. M., & van de Ven, T. G.** (2020). A review on surface-functionalized cellulosic nanostructures as biocompatible antibacterial materials. *Nano-Micro Letters*, *12*(1), 1-23.

[4] **Habibi, Y.** (2014). Key advances in the chemical modification of nanocelluloses. Chemical Society Reviews, 43(5), 1519-1542.

[5] **Le Gars, M., Bras, J., Salmi-Mani, H., Ji, M., Dragoe, D., Faraj, H., ... & Roger, P.** (2020). Polymerization of glycidyl methacrylate from the surface of cellulose nanocrystals for the elaboration of PLA-based nanocomposites. *Carbohydrate polymers*, *234*, 115899.

[6] **Shankaran, D. R.** (2018). Cellulose nanocrystals for health care applications. In *Applications of nanomaterials* (pp. 415-459). Woodhead Publishing

[7] **Trache, D., Tarchoun, A. F., Derradji, M., Hamidon, T. S., Masruchin, N., Brosse, N., & Hussin, M. H.** (2020). Nanocellulose: from fundamentals to advanced applications. *Frontiers in Chemistry*, *8*, 392.

[8] **Habibi, Y., Lucia, L. A., & Rojas, O. J.** (2010). Cellulose nanocrystals: chemistry, self-assembly, and applications. *Chemical reviews*, *110*(6), 3479-3500.

[9] **Petersson, L., Kvien, I., & Oksman, K.** (2007). Structure and thermal properties of poly (lactic acid)/cellulose whiskers nanocomposite materials. *Composites Science and Technology*, *67*(11-12), 2535-2544

[10] **Hathaway, B. A.** (1992). Organic Chemistry, (Solomons, TW Graham).

[11] **Trinh, B. M., & Mekonnen, T.** (2018). Hydrophobic esterification of cellulose nanocrystals for epoxy reinforcement. Polymer, 155, 64-74.

[12] **Ramírez, J. A. Á., Fortunati, E., Kenny, J. M., Torre, L., & Foresti, M. L.** (2017). Simple citric acid-catalyzed surface esterification of cellulose nanocrystals. *Carbohydrate polymers*, *157*, 1358-1364.

[13] **Spinella, Stephen, et al.** "Polylactide/cellulose nanocrystal nanocomposites: Efficient routes for nanofiber modification and effects of nanofiber chemistry on PLA reinforcement." *Polymer* 65 (2015): 9-17.

[14] **Wei, L., Agarwal, U. P., Hirth, K. C., Matuana, L. M., Sabo, R. C., & Stark, N. M.** (2017). Chemical modification of nanocellulose with canola oil fatty acid methyl ester. *Carbohydrate polymers*, *169*, 108-116.

[15] **Thangarasu, V., & Anand, R.** (2019). Comparative evaluation of corrosion behavior of Aegle Marmelos Correa diesel, biodiesel, and their blends on aluminum and mild steel metals. In Advanced biofuels (pp. 443-471). Woodhead Publishing.

[16] **Lang, X., Dalai, A. K., Bakhshi, N. N., Reaney, M. J., & Hertz, P. B.** (2001). Preparation and characterization of bio-diesels from various bio-oils. Bioresource technology, 80(1), 53-62.

[17] **Khanjanzadeh, H., Behrooz, R., Bahramifar, N., Gindl-Altmutter, W., Bacher, M., Edler, M., & Griesser, T.** (2018). Surface chemical functionalization of cellulose nanocrystals by 3-aminopropyltriethoxysilane. *International journal of biological macromolecules*, *106*, 1288-1296.

[18] **Le Gars, M., Delvart, A., Roger, P., Belgacem, M. N., & Bras, J.** (2020). Amidation of TEMPO-oxidized cellulose nanocrystals using aromatic aminated molecules. Colloid and Polymer Science, 298(6), 603-617.

[19] **Pal, N., Banerjee, S., Roy, P., & Pal, K.** (2019). Reduced graphene oxide and PEG-grafted TEMPO-oxidized cellulose nanocrystal reinforced poly-lactic acid nanocomposite film for biomedical application. *Materials Science and Engineering: C*, *104*, 109956.

[20] **Fraschini, C., Chauve, G., & Bouchard, J.** (2017). TEMPO-mediated surface oxidation of cellulose nanocrystals (CNCs). *Cellulose*, *24*(7), 2775-2790.

[21] **Chen, Q. J., Zhou, L. L., Zou, J. Q., & Gao, X.** (2019). The preparation and characterization of nanocomposite film reinforced by modified cellulose nanocrystals. *International journal of biological macromolecules*, *132*, 1155-1162.

[22] **de Oliveira Taipina, M., Ferrarezi, M. M. F., Yoshida, I. V. P., & do Carmo Gonçalves, M. (2013). Surface modification of cotton nanocrystals with a silane agent. Cellulose, 20(1), 217-226.**

[23] **Siqueira, G., Bras, J., Follain, N., Belbekhouche, S., Marais, S., & Dufresne, A. (2013).** Thermal and mechanical properties of bio-nanocomposites reinforced by Luffa cylindrica cellulose nanocrystals. Carbohydrate polymers, 91(2), 711-717.

[24] **Follain, N., Belbekhouche, S., Bras, J., Siqueira, G., Marais, S., & Dufresne, A. (2013).** Water transport properties of bio-nanocomposites reinforced by Luffa cylindrica cellulose nanocrystals. Journal of membrane science, 427, 218-229**.**

[25] **Geurds, L., Lauko, J., Rowan, A. E., & Amiralian, N.** (2021). Tailored nanocellulose-grafted polymer brush applications. *Journal of Materials Chemistry A*, *9*(32), 17173-17188.

[26] **Tang, C., Spinney, S., Shi, Z., Tang, J., Peng, B., Luo, J., & Tam, K. C.** (2018). Amphiphilic cellulose nanocrystals for enhanced Pickering emulsion stabilization. *Langmuir*, *34*(43), 12897-12905.

[27] **Zhang, C., Salick, M. R., Cordie, T. M., Ellingham, T., Dan, Y., & Turng, L. S.** (2015). Incorporation of poly (ethylene glycol) grafted cellulose nanocrystals in poly (lactic acid) electrospun nanocomposite fibers as potential scaffolds for bone tissue engineering. *Materials Science and Engineering: C*, *49*, 463-471.

[28] **Zheng, T., Clemons, C. M., & Pilla, S.** (2021). Grafting PEG on cellulose nanocrystals via polydopamine chemistry and the effects of PEG graft length on the mechanical performance of composite film. Carbohydrate Polymers, 271, 118405.

[29] **Araki, J., Wada, M., & Kuga, S.** (2001). Steric stabilization of a cellulose microcrystal suspension by poly (ethylene glycol) grafting. *Langmuir*, *17*(1), 21-27.

[30] **Azzam, F., Heux, L., Putaux, J. L., & Jean, B.** (2010). Preparation by grafting onto, characterization, and properties of thermally responsive polymer-decorated cellulose nanocrystals. *Biomacromolecules*, *11*(12), 3652-3659.

[31] **Ribeiro, P. L. L., Figueiredo, T. V. B., Moura, L. E., & Druzian, J. I.** (2019). Chemical modification of cellulose nanocrystals and their application in thermoplastic starch (TPS) and poly (3-hydroxybutyrate)(P3HB) nanocomposites. *Polymers for Advanced Technologies*, *30*(3), 573-583.

[32] **Spinella, S., Samuel, C., Raquez, J. M., McCallum, S. A., Gross, R., & Dubois, P.** (2016). Green and efficient synthesis of dispersible cellulose nanocrystals in biobased polyesters for engineering applications. *ACS Sustainable Chemistry & Engineering*, *4*(5), 2517-2527.

[33] **Kedzior, S. A., Graham, L., Moorlag, C., Dooley, B. M., & Cranston, E. D.** (2016). Poly (methyl methacrylate)-grafted cellulose nanocrystals: One-step synthesis, nanocomposite preparation, and characterization. *The Canadian Journal of Chemical Engineering*, *94*(5), 811-822.

[34] **Sessini, V., Navarro-Baena, I., Arrieta, M. P., Dominici, F., López, D., Torre, L., ... & Peponi, L.** (2018). Effect of the addition of polyester-grafted-cellulose nanocrystals on the shape memory properties of biodegradable PLA/PCL nanocomposites. *Polymer Degradation and Stability*, *152*, 126-138

[35] **Vatansever, E., Arslan, D., Sarul, D. S., Kahraman, Y., Gunes, G., Durmus, A., & Nofar, M.** (2020). Development of CNC-reinforced PBAT nanocomposites with reduced percolation threshold: A comparative study on the preparation method. *Journal of Materials Science*, *55*(32), 15523-15537.

CURRICULUM VITAE

Name Surname **:** Onur Nuri ARSLAN

EDUCATION

- **B.Sc.** **:** 2020, Istanbul Technical University, Faculty of Chemical and Metallurgical Engineering, Metallurgical and Materials Engineering Department
- **B.Sc.** **:** 2022, Istanbul Technical University, Faculty of Science and Letters, Chemistry Department

PUBLICATIONS, PRESENTATIONS AND PATENTS ON THE THESIS:

- **Arslan, O. N.,** Gunturkun, D., Bekem, A., Alkan Goksu, Y., Nofar. M. "Surface Modified Cellulose Nanocrystal Incorporated Nanocomposite" International Graduate Research Symposium
- **Arslan, O.N.,** Goksu, Y. A., Nofar, M., "Biodegradable polymer nanocomposites using modified cellulose nanocrystals", 21st International Metallurgy and Materials Congress (IMMC 2022), Istanbul Turkey, Sep 6-8, 2022

OTHER PUBLICATIONS, PRESENTATIONS AND PATENTS:

- **Arslan, O. N.,** Gunturkun, D., Ozdemir, B., Bekem, A., Alkan Goksu, Y., Nofar. M. "Surface Modification of Cellulose Nanocrystal (CNC) and its Dispersion in PLA matrix", EPF European Polymer Congress (EPF 2022), Prague, Czechsia, June 26 - July 1, 2022